DEPARTMENT OF STATISTICS
University of Wisconsin
1210 West Dayton St.
Madison, WI 53706

TECHNICAL REPORT NO. 1010
July 13, 1999

Quantitative Study of Smoothing Spline-ANOVA Based Fingerprint Methods for Attribution of Global Warming

Alan Chiang
Department of Statistics, University of Wisconsin, Madison WI

Grace Wahba
Department of Statistics, University of Wisconsin, Madison WI

Joseph Tribbia
National Center for Atmospheric Research

Donald R. Johnson
Space Sciences and Engineering Center, University of Wisconsin, Madison WI

Quantitative Study of Smoothing Spline-ANOVA Based Fingerprint Methods for Attribution of Global Warming [1]

Alan Chiang [2]
Department of Statistics, University of Wisconsin, Madison WI
Grace Wahba [3]
Department of Statistics, University of Wisconsin, Madison WI
Joseph Tribbia[4]
National Center for Atmospheric Research
Donald R. Johnson [5]
Space Science and Engineering Center, University of Wisconsin, Madison WI

Key words and phrases. Fingerprint methods for climate change detection and attribution. Smoothing spline ANOVA. Partial spline models. Detection of signal in noise. Monte Carlo and Bayes methods for reference distributions.

July 13, 1999

Contents

[1]Corresponding author address: Prof. Grace Wahba, Department of Statistics, University of Wisconsin, 1210 W. Dayton St., Madison WI 53706.

[2]Research supported in part by NASA Grant NAG5 3769 and NSF Grant DMS9121003
[3]Research supported in part by NASA Grant NAG5 3769 and NSF Grant DMS 9704758
[4]Research supported by the Geophysical Statistics Project under NSF Grant DMS93122686
[5]Research supported in part by NASA Grants NAG5 3769 and NAG5 4398 and DOE Grant DE-FG02-92ER61439

Abstract

A fingerprint-based method for climate change detection and attribution with some novel features is proposed. The method is based on a functional ANOVA (ANalysis Of VAriance) decomposition of a time and space signal, further decomposed into global time-trend and time-trend anomaly as a function of space. The method estimates the signal as a component of forced minus background climate model output, and then uses a partial spline model to estimate and test for the existence of signal in historical data. The method is based on the classical detection of signal in noise, however there are several features apparently novel to the fingerprint literature, in particular, the analysis takes place directly in observation space, anomalies are fitted directly and there is possibility for estimating certain parameters of covariance models for the historical data as part of the analysis. Simulation studies using climate model runs from GFDL and NCAR and historical data for NH Winter average surface temperature for the period 1961-90 suggest that the linear component of the time trend anomaly has the potential for strong detection and attribution, but by analyzing simulated data forced with a GFDL signal, and tested via an NCAR signal, it is made clear that more accurate climate model output for this signal, than that used in this study, is needed to realize these benefits. The method generalizes to include a vertical dimension and indirect observations, and to the examination of spatially varying time trends and drifts in observed minus forecast data in forecast models.

1 Introduction

In this paper, fingerprint methods based on an ANOVA decomposition of the time and space varying historical NH Winter average surface temperature are developed. The ANOVA decomposition, which is a function space analogue of the discrete ANOVA (ANalysis of VAriance) decomposition familiar in introductory statistics courses, decomposes a function defined on time and space into a grand mean, a main effect for time, a main effect for space, and an interaction term. This decomposition is then further broken down to include the linear component of the main effect for time (linear component of the global time trend), and the linear component of the time trend spatial anomaly. The terms in the ANOVA decomposition are then estimated from observations scattered in space and time by solving a smoothing spline like variational problem. Here NH winter (DJF) average surface temperature as a function of year (1961-90) and position (latitude, longitude) is examined, but dependency on a vertical coordinate may also be considered, and various other observation functionals, including indirect ones such as satellite radiances may be included via a slight generalization. The approach here allows for varying kinds of fingerprints based on components of this decomposition, including simple (here linear component of the global time trend) and relatively complex (here linear component of the time trend spatial anomaly).

The choice of the pair of these fingerprints for study was based on Hegerl, von Storch, Hasselmann, Santer, Cubash & Jones (1996), who looked at the time trend of the surface temperature, as a function of space. Many other fingerprints have been studied by various authors, and we discuss later how other fingerprints may be considered via the methods proposed here. The method here is based on the smoothing spline ANOVA decomposition of Luo, Wahba & Johnson (1998) to extract a signal from climate model output, and then the method being proposed uses the theory of partial spline models (Wahba (1990)) to estimate signal strength in the historical data. A fingerprint due to forcing is extracted from forced minus background climate model runs, and then hypotheses tests are carried out concerning the existence/strength of the signal in the historical data. The tests are carried out using estimates of the variability of the test statistic(s) due to the natural variability of the climate plus observational and subgrid scale noise. In this paper the variability estimates of the test statistics are obtained in two different ways. The first uses a sequence of climate model background runs, some forced runs, and realistic estimates of the subgrid scale observational noise to simulate sets of background and forced observational data, and these data sets are used to obtain Monte Carlo estimates of the distributions of the test statistics. The second method uses the relationship between variational problems and Bayes estimates to identify the tuning parameters in the variational problem that have been obtained from the data with variance ratios, and then to compute theoretical test statistic variances based on them.

There are several more or less unique features of the approach here, although, like most fingerprint methods, it has as its core classical signal in noise hypothesis tests. The novel features include: climate model output is brought to observation space, rather than observations brought to model grid point space; familiar atmospheric anomalies are modeled specifically in a functional (smoothing spline) ANOVA decomposition, which handles irregular observations in both time and space in a fairly natural way; covariances are modeled with a very sparse parameterization, with the parameters being estimated from the data

simultaneously with the test statistics, and the setup allows the generation of climate model variability either via climate model runs, or from the modeled covariances. A variety of signals can be handled within the paradigm proposed here.

A computational algorithm is developed here, signals are extracted from five different 1961-1990 forced and background climate model runs, natural variability is estimated, and hypotheses that the historical record contains the signals are tested.

The two kinds of fingerprints considered here are at opposite ends of the complexity spectrum. The first 'fingerprint', the linear component of the global time trend, (that is, the average rate of change of the global mean temperature over the time span considered), is a signal with one degree of freedom. The second, the linear component of the spatial anomaly of the time trend is much more complex. It is a spatial pattern that has a number of degrees of freedom which is a moderate fraction of the number of observing stations, which is 1000 in this paper.

This paper does not answer the question: Is there a highly statistically significant test result that the observed warming is unlikely to have been generated by natural variability? Rather it is observed here (as well as elsewhere) that by using a simple fingerprint the historical data is more consistent with forced climate model output than with background climate model output (at least for that used in the present study.) But there is a moderate amount of variability in the 'simple' statistic , as generated by background variability in the 1000 year background run used here. It appears that the use of this simple statistic will have to await a stronger signal before rejecting the no-signal hypothesis at, say, a P-value of .000001. Furthermore it is shown here, via observational data simulated from both forced and background climate runs, that *if* the complex signal used here is known highly accurately, then the distributions of the test statistic under the null hypothesis that there is no signal vs the alternative that the specified signal is present, are well separated, and strong attribution results would be possible via the present methods. However, this is a rather big 'if'. The very specific complex patterns generated by our forced and background climate runs were not found here in the historical data. However, when simulated observational data using a complex signal from one forced climate run was analyzed using the signal from a similar forced climate run from a different climate model, only weak separation of the signal and no signal distributions were obtained. That is, the power of this 'high powered' test is very much degraded by a simulated model error that is no doubt a lower bound on actual model error. We are left with the conclusion (with various caveats based on limitations of the present study, as well as some possibly strong assumptions concerning the reasonableness of additive linear approximations to change due to forcing) (Ramaswamy & Chen (1997)) that if more accurate climate model signal output were available, the potential is there for much more powerful level of attribution than is possible with the simpler fingerprint at the present time. We observe that is a tradeoff between using a complex signal, which has strong potential for distinguishing signal from natural variability, and the more stringent requirements on climate model accuracy to provide such a signal. Remarks concerning this tradeoff have previously been made, for example, by Hegerl & North (1997).

There are many recent research works on methods for climate change detection and attribution. Recent reviews and overview papers related to fingerprint methods include Levine & Berliner (1999), Zwiers (1998), Hasselmann (1998). Recent papers on fingerprint and

related signal-in-noise detection include: Barnett, Hegerl, Santer & Taylor (1998), Goody, Anderson & North (1998), Haigh (1996), Hasselmann (1997), Hegerl, Hasselmann, Cubash, Mitchell, Roeckner, Voss & Waszkewitz (1997), Hegerl & North (1997), Hegerl et al. (1996), Leroy (1998), Leroy (1999), North, Kim, Shen & Hardin (1995), North & Stevens (1998*a*), Santer, Taylor, Wigley, Penner, Jones & Cubasch (1995), Santer, Taylor, Wigley, Johns, Jones, Karoly, Mitchell, Oort, Penner, Ramaswamy, Schwarzkopf, Stouffer & Tett (1996), Stott & Tett (1998), Stevens & North (1996), Tett, Mitchell, Parker & Allen (1996), von Storch & Zwiers (1999), Wigley, Jaumann, Santer & Taylor (1998).

In Section 2 the historical and climate model information that is used in this study is described. In Section 3 the mathematical foundations of the approach are presented, including descriptions of the smoothing spline ANOVA and partial spline models to test for the existence of a signal, and the relation of these objects to Bayes estimates and fingerprinting. The computational algorithm is a generalization of that used in Luo et al. (1998) and described in detail in Luo (1998) and Wahba & Luo (1997). The generalization of the algorithm to fingerprinting is briefly described in this section. The method used to carry over gridded climate output to the observing points in time and space, and the ANOVA decomposition of the carried over model output is described in Appendix A. In Section 4 the results of several fingerprinting experiments are described. Signal and test statistic reference distributions were generated from long-run climate model output by Monte Carlo methods, and used to analyze historical data. The experiment simulating observations from one climate model (in observation space) and using signal from another climate model to examine the effects of an erroneous signal is described. The reference distributions obtained by Monte Carlo methods from climate runs are compared with theoretical test statistic variances obtained by simultaneously fitting certain covariance parameters along with the hypothesis tests. The results of this comparison were mixed but somewhat encouraging. In Section 5 tradeoffs between requirements for strong separation between forced and background test statistic distributions, and requirements for model accuracy are discussed. Section 6 discusses a number of generalizations, including more general time-space covariance models than those used in the present work, and extensions of the approach to include the vertical dimension and indirect (satellite) observations. Other possible applications, in particular to the study of observed - forecast biases, trends or drifts are also noted. Section 7 is a summary and conclusions.

2 The historical data and climate model output

2.1 The historical data

This study used the monthly mean historical surface temperature records converted to NH winter (DJF) means archived in the in the Global Historical Climatology Network (GHCN). The winter means were used only when all three of DJF observations were available. The data were obtained from http://www.ncdc.noaa.gov/ol/climate/research/ghcn/ghcn.html. The data set used was extracted in January 1998. This site has moved to http://www.ncdc.noaa.gov/ol/climatedata.html. A sample of 1000 stations for 30 years (1961-1990) was selected. The stations in this report were selected to match that in Luo et al. (1998), which had used an earlier version of the GHCN data set. However only 947 of the stations used there

were available from the version available in January 1998. Then 53 stations were chosen deliberately so that the 1000 stations are distributed as uniformly as possible on the sphere. The black dots in Figure 5 and subsequent figures show the locations of these 1000 stations. If a report had been available for every station at each of the thirty years, there would have been 30 000 observation points, in fact not every station had complete data for every winter, and there were only $n = 23\ 119$ data points distributed in time and space. We believe that the stations chosen are fairly representative. The numerical values of estimated global temperature may change somewhat if the station distribution were changed in a material way, however, due to the fact that in this study, the climate model output is extrapolated to the data points, we believe the conclusions here are relatively insensitive to minor changes in the data distribution, and would not change much if the available observations from all the stations reporting in the given period were used. See for example Wang & Shen (1999).

2.2 The climate model runs

In this study climate model runs from the Geophysical Fluid Dynamics Laboratory (GFDL) which are as of June 1999 available at http://www.gfdl.gov/gfdl_research.html were used. To obtain the 'signal' part of a 100 year run in which the CO_2 concentration in the atmosphere was increased by 1% per year (compounded) was used. This will be called the "forced run". The model control run was also used. This was a 1000 year run with greenhouse gases in a steady state. This will be called the "background run". Year 1 for the GFDL runs was 1958. These runs were used beginning with NH winter 1960-1961. The GFDL 'signal' used here is based on the difference between the forced run and a corresponding segment of the background run. The remainder of the background run was chopped up into 29 disjoint 30-year pieces and each piece used to simulate 30 years of "background noise". Although these pieces are not independent, the convenient fiction was adopted that it was reasonable to treat them as independent in the applications described here. The GFDL model has been described in detail in Manabe, Stouffer, Spelman & Bryan (1991) and Manabe, Spelman & Stouffer (1992).

Four other signals were extracted from climate model experiments done at the National Center for Atmospheric Research (NCAR) and provided courtesy of Jerry Meehl. The experiments were performed with a global coupled GCM to include the indirect forcing effect of sulfate aerosols in combination with transient greenhouse gas forcing and the direct effect of sulfate aerosols, and are described in detail in Meehl, Washington, Erickson, Briegleb & Jaumann (1996).

The first experiment was a 75 year experiment with CO_2 increasing at 1% per year compounded relative to a reference CO_2 amount of 330 ppm in the background experiment, (called "CO_2-only" in Meehl et al. (1996)). The second is a 75 year experiment with the CO_2-only forcing plus the direct effect of sulfate aerosols ("1Xdirect"). The third is a 75 year experiment configured in the same way as 1Xdirect except that the time-evolving forcing of the sulfate aerosol direct effect is doubled ("2Xdirect"). The fourth experiment ("direct+indirect") uses the time evolving forcing from the 1Xdirect experiment, and adds the time-evolving forcing from an estimate of the indirect effect of sulfate aerosols derived from Erickson, Oglesby & Marshall (1995). These four runs are labeled NCAR1, NCAR2,

NCAR3 and NCAR4 in what follows. Only the same 30-year (1961-1990) winter temperature simulations from both GFDL and NCAR models were taken for comparison. Both the GFDL and NCAR model simulations are produced on a 48-by-40 Gaussian grid. Figures 1 and 2 give the GFDL and NCAR1 forced run mean of the 30 year average winter temperature at each of the 1,920 grid points. Figures 3 and 4 give the 'signal' linear component of the spatial time trend temperature in model grid point space for the GFDL and NCAR1 model output. 'Signal' here means the forced minus the corresponding background run. This was obtained as follows: First, at each grid box, the 30 years x 1920 temperatures of the background run are subtracted from the forced run. Then at each grid box, a least squares straight line is fit to the 30 years of forced minus background temperature differences. The slope of this line, plotted in degrees Centigrade per year, is taken as the trend due to forcing, and that is what is plotted. It can be seen that the NCAR plot gives a cooling trend over Greenland, a strong warming trend over Siberia and Australia, and so forth.

2.3 ANOVA decomposition of the historical data and the climate model output

Figures 5 through 14 are based on a smoothing spline ANOVA fit and decomposition of the historical data, and the corresponding ANOVA decomposition of the GFDL and NCAR forced run after being carried over (quasi-interpolated) to the $n = 23\ 119$ observational data points. The plots are obtained from components of the ANOVA decompositions, to be reviewed in the next section. The carrying over of the climate model output to the observational points renders the model output more directly comparable to the observational data, and is believed to involve fewer assumptions than carrying the observational data to the model grid points. Figure 5 gives the 30 year average temperature, based on the 23 119 values of the GFDL forced run obtained from carrying over the GFDL gridded data to the observational data points, and then computing an ANOVA decomposition for these 'observational' points, and figure 6 is the same plot for the NCAR1 forced run. Figures 5 and 6 are to be compared with Figures 1 and 2. It can be seen that there is some distortion of the gridded output, primarily, the irregular observations induce an artifactual high where there are no 'observations' just east of Central America, that does not exist in the gridded data. Otherwise the extrapolation beyond the observation points in Figures 5 and 6 appear to be quite good. Figure 7 gives the historical 30 year average temperature, based on the 23 119 historical data points, using the same ANOVA decomposition as was used to obtain Figures 5 and 6. The only difference in the analysis of climate model quasi-interpolated data and historical data, is that the amount of smoothing of the climate model data is based on the number of significant figures in the climate model output, (as described in Appendix A.2) while the smoothing for the observational data is based on an estimated size of the subgrid scale white noise in the observations, obtained via generalized cross validation (GCV). It can be seen that in the neighborhoods of the observing stations the gridded climate model output, the climate model output as seen through the 'eyes' of the time and location of the historical data points, and the historical data, is in rough agreement, although the NCAR1 average temperatures are warmer than the historical average temperatures which are in turn warmer than the GFDL temperatures. Figure 8 gives the global NH winter mean temperature as

a function of year for the historical data, panel (a); and for the five forced climate runs, GFDL forced, (b); and NCAR1, NCAR2, NCAR3 and NCAR4 (c)-(f). These estimates of global average winter temperature are based on an ANOVA decomposition which includes averaging over the entire sphere. As a consequence, for example, the average of the 29 points in Figure 8, panel (a) (mathematically) equals the integral (in spherical coordinates) over Figure 7. The global averages in Figure 8 panel (a) are warmer than the land average temperatures computed in Luo et al. (1998), which represent an integral over the land areas of Figure 7.

Figure 9 gives the estimated 1961-1990 30 year average rate of change of temperature as a function of latitude and longitude for the historical data. Figures 10 through 14 give the corresponding 'signal' plots for the GFDL and NCAR1 through NCAR4. Here 'signal' means the difference between the average rate of change of the forced runs and the background runs, as a function of space. The plots are left blank where there is no observing station within 500 km. Figures 10 and 11 may be compared to Figures 3 and 4. Figures 10 and 11 represent a slightly distorted view of the average rate of change of the temperature as a function of space of Figures 3 and 4, distorted by being seen through the 'eyes' of the observing system. We will be comparing the information in the historical plot with the information in the corresponding climate model plots 10 through 14.

3 Smoothing spline ANOVA models, partial spline models, Bayes estimates and fingerprinting

3.1 Functional ANOVA decompositions and anomalies

A functional ANOVA decomposition is a decomposition of a function of two (or more) variables on a tensor product domain with components grand mean, main effects, and two (or more) factor interactions. This rather abstract definition will be seen to fit in nicely with the usual notion of anomalies in atmospheric sciences. More details may be found in Luo et al. (1998), and more generally in Wahba, Wang, Gu, Klein & Klein (1995) in other contexts. Details for the case of this paper will be given. The two variables will be the year index time, $t \in \{1, 2, .., n_1\}$ ($n_1 = 30$), and the location index $P = (latitude, longitude) \in \mathcal{S}$, where $\mathcal{S}$ is the sphere. Hence the domain of the meteorological field is $\{1, 2, .., n_1\} \times \mathcal{S}$. Note that one variable is discrete and the other continuous, even though observations exist at only a finite number of locations in $\mathcal{S}$. Define time and space averaging operators as follows:

$$\mathcal{E}_t f(t, P) = \frac{1}{n_1} \sum_{t=1}^{n_1} f(t, P)$$

$$\mathcal{E}_P f(t, P) = \frac{1}{4\pi} \int_{\mathcal{S}} f(t, P) dP.$$

Consider a direct sum decomposition of the identity operator defined in the following manner:

$$I = (\mathcal{E}_t + (I - \mathcal{E}_t))(\mathcal{E}_P + (I - \mathcal{E}_P)) = \mathcal{E}_t\mathcal{E}_P + (I - \mathcal{E}_t)\mathcal{E}_P + \mathcal{E}_t(I - \mathcal{E}_P) + (I - \mathcal{E}_t)(I - \mathcal{E}_P). \quad (1)$$

Then any function on our domain has a unique decomposition of the form

$$f(t,P) = d_1 + g_1(t) + g_2(P) + g_{12}(t,P),$$

given by $d_1 = \mathcal{E}_t\mathcal{E}_P f, g_1(t) = (1-\mathcal{E}_t)\mathcal{E}_P f, g_2(P) = \mathcal{E}_t(I-\mathcal{E}_P)f, g_{12}(t,P) = (I-\mathcal{E}_t)(I-\mathcal{E}_P)f$, and these component functions satisfy the following conditions:

$$\mathcal{E}_t g_1 = \mathcal{E}_t g_{12} = \mathcal{E}_P g_2 = \mathcal{E}_P g_{12} = 0.$$

If the linear time trend is of interest, another another operator can be defined to single out the time trend by defining $\phi(t) = t-(n_1+1)/2$ and letting $\mathcal{E}'_t$ be the operator which projects any function of t along ϕ, $(\mathcal{E}'_t f)(t,P) = \frac{\sum_{t'=1}^{n_1} f(t',P)\phi(t')}{\sum_{t'=1}^{n_1}\phi^2(t')}\phi(t)$. Decomposing g_1 and g_{12} via $(\mathcal{E}'_t + (I-\mathcal{E}'_t))$ results in the decomposition of f as

$$f(t,P) = d_1 + d_2\phi(t) + f_1(t) + f_2(P) + f_{\phi,2}(P)\phi(t) + f_{12}(t,P). \tag{2}$$

The component functions of f then satisfy the following moment conditions

$$\sum_{t=1}^{n_1} f_1(t) = \sum_{t=1}^{n_1} f_1(t)\phi(t) = \sum_{t=1}^{n_1} f_{12}(t,P) = \sum_{t=1}^{n_1} f_{12}(t,P)\phi(t) = 0 \tag{3}$$

$$\int_{\mathcal{S}} f_2(P)dP = \int_{\mathcal{S}} f_{\phi,2}(P)dP = \int_{\mathcal{S}} f_{12}(t,P)dP = 0 \tag{4}$$

for all t and P. See Wahba (1990), Gu & Wahba (1993) and Luo et al. (1998) for details about formulating such ANOVA models. It is clear that these components are climatologically meaningful. d_1 is the grand mean of average winter temperature; d_2 is the linear trend coefficient of the global average winter temperature; $d_1 + d_2\phi(t) + f_1(t)$ is the global average winter temperature history; $d_1 + f_2(P)$ is the average winter temperature at location P; $d_2 + f_{\phi,2}(P)$ is the linear trend coefficient of the average winter temperature at location P; and $d_2\phi(t) + f_1(t) + f_{\phi,2}(P)\phi(t) + f_{12}(t,P)$ can be considered the anomaly at (t,P) over the time average at P. Figures 5, 6 and 7 are $d_1 + f_2(P)$, Figure 8 is $d_1 + d_2\phi(t) + f_1(t)$ and Figures 9 through 14 are $d_2 + f_{\phi,2}(P)$. Note that $(d_2 + f_{\phi,2}(P))$ is the coefficient of ϕ and $\int f_{\phi,2}(P)dP = 0$; thus $f_{\phi,2}(P)$ is the coefficient of the linear component of the spatial anomaly of the time trend.

3.2 SS-ANOVA fits

Suppose the observations satisfy

$$y_i = f(t_i, P_i) + \epsilon_i, i = 1, 2, \cdots, n \tag{5}$$

were the ϵ_i represent uncorrelated 'noise' that is, independent measurement errors and/or sub grid scale phenomena, assumed to be approximately Gaussian, $\epsilon_i \sim \mathcal{N}(0,\sigma^2)$, for some σ^2. A smoothing spline ANOVA estimate f_θ is an estimate of the components $d_1, d_2, f_1, f_2, f_{\phi,2}$

and f_{12} obtained by finding them in an appropriate space[6] to minimize

$$\sum_{i=1}^{n}(y_i - f(t_i, P_i))^2 + J_\theta(f) \tag{6}$$

where $J_\theta(f) = \theta_1^{-1}J_1(f_1) + \theta_2^{-1}J_2(f_2) + \theta_3^{-1}J_3(f_{\phi,2}) + \theta_4^{-1}J_4(f_{12})$. $f(t, P)$ in (6) is as in (2), and the J's are suitably defined quadratic penalty functionals[7] which constrain the functions to be 'smooth' in some sense. Some common choices of the J's are the scattered data equivalent to imposing a low-pass (Butterworth) filter on the observations. In this paper $J_1(f_1) = \sum_{t=1}^{n_1-2}(f_1(t+2) - 2f_1(t+1) + f_1(t))^2$, J_2 and J_3 are the same, and are topologically equivalent to $\int_{\mathcal{S}}(\Delta f)^2 dP$, where Δ is the Laplacian on the sphere, and J_4 is derived from J_1 and J_2 as the squared norm of the corresponding tensor product space. Some other choices of penalty functionals are noted in Section 6.1.

Letting f_θ be the minimizer of (6), it is known that f_θ has a representation in terms of $n+2$ basis functions:

$$f_\theta(t, P) = d_1 + d_2\phi(t) + \sum_{i=1}^{n} c_i Q_\theta(t, P; t_i, P_i) \tag{7}$$

where n of these basis functions are defined by

$$Q_\theta(t, P; t'P') = \sum_{v=1}^{4} \theta_v R_v(t, P; t', P'), \quad (t', P') = (t_i, P_i), i = 1, \cdots, n. \tag{8}$$

The $Q_\theta(\cdot, \cdot; t_i, P_i)$ $i = 1, \cdots n$ are known as representers. Here the R_v are positive definite functions (covariances) associated with the J_v's, and for later reference are reproduced from Luo et al. (1998) in Table 6. The four penalized terms $f_1, f_2, f_{\phi,2}$ and f_{12} can be identified with the four terms on the right hand side of (8) and easily extracted once $c = (c_1, \cdots, c_n)$ is given, see Appendix A.1. Note that the representers satisfy the relevant moment conditions (3). A Smoothing spline ANOVA fit to a 30 year, 1000 station subset of an earlier version of the GHCN data set, similar to the data set used here, was obtained in Luo et al. (1998), using an algorithm noted in Luo et al. (1998), and given in Wahba & Luo (1997) and further developed in Luo (1998) (to be called the LW algorithm). The LW algorithm does not involve inverting or decomposing large $(n \times n)$ matrices, this is avoided via a combination of backfitting, EM-like imputation and randomized trace methods. The LW algorithm will be used directly and as a subroutine.

3.3 SS-ANOVA fits with signal (partial spline model)

In the fingerprint method focus is on the possible existence of particular patterns characteristic of the effects of increased greenhouse gases, in the historical data. It is assumed that interest is in a signal which is some linear combination of signals $\sum_{k=1}^{p}\alpha_k S_k(t, P) \equiv S(t, P)$, where

[6]The space will be a reproducing kernel Hilbert space, see Wahba (1990) but that concept is not needed for the discussion here.

[7]They are squared norms in a reproducing kernel Hilbert space.

the S_k are given. The signal will be added to the decomposition (2), and $\alpha = (\alpha_1, \cdots, \alpha_p)$ estimated, as part of the variational problem (6). That is, the observations are modeled as

$$y_i = \sum_{k=1}^{p} \alpha_k S_k(t_i, P_i) + f(t_i, P_i) + \epsilon_i, \tag{9}$$

where $f(t, P)$ is as in (2) and ϵ_i is as before. Now, it is desired to find α and f to minimize

$$\sum_{i=1}^{n} (y_i - \sum_{k=1}^{p} \alpha_k S_k(t_i, P_i) - f(t_i, P_i))^2 + J_\theta(f). \tag{10}$$

This is an example of a partial spline model as discussed in Wahba (1990) and elsewhere. The minimizer f_θ is known to have a representation as in (7). The unknowns α and d and c can be obtained via an iteration between a pth order least squares step and the LW algorithm as follows: Let $A_{(0)}(\theta)$ be the influence matrix for the minimizer of (6), that is, if f_θ is the minimizer of (6), then $A_{(0)}(\theta)$ satisfies

$$\begin{pmatrix} f_\theta(t_1, P_1) \\ \vdots \\ f_\theta(t_n, P_n) \end{pmatrix} = A_{(0)}(\theta) y. \tag{11}$$

Let S be the $n \times p$ matrix with ikth entry $S_k(t_i, P_i)$. Then, letting $\bar{f}_\theta$ stand for the vector on the left of (11), if $\bar{f}_\theta$ is given, then α must satisfy

$$S'S\alpha = S'(y - \bar{f}_\theta), \tag{12}$$

and, if α is given, then f_θ must satisfy

$$\bar{f}_\theta = A_{(0)}(\theta)(y - S\alpha). \tag{13}$$

Thus an iterative procedure can be carried out alternating between least squares and the LW algorithm, and it can be shown to converge under general conditions provided that the S_k are linearly independent and linearly independent of the constant function and ϕ over the observation points.

3.3.1 Estimation of θ and σ^2

For data following the models (5) and (9) where it was assumed that there is 'white noise' of nontrivial magnitude added to a 'smooth' signal the four components of θ were chosen by minimizing the GCV function $V(\theta)$. For (6) $V(\theta) = \frac{\frac{1}{n}\|y - \bar{f}_\theta\|^2}{(\frac{1}{n} trace(I - A_{(0)}(\theta)))^2}$ and for (10) $V(\theta) = \frac{\frac{1}{n}\|y - S\alpha - \bar{f}_\theta\|^2}{(\frac{1}{n} trace(I - A(\theta)))^2}$, where $A(\theta)$ is the influence matrix for the problem (10), that is, the matrix satisfying $\bar{f}_\theta + S\alpha = A(\theta)y$. $TraceA_{(0)}(\theta)$ and $traceA(\theta)$ were estimated by the same randomized trace technique used in Luo et al. (1998), Girard (1998), for a sequence of θ's, and $V(\theta)$ minimized as a function of four variables by the downhill simplex method (Nelder & Mead (1965)). The variance σ^2 of the ϵ_i is estimated by the residual sum of squares divided by the degrees of freedom for signal, (Wahba (1983)) $\hat{\sigma}^2 = \frac{\|y - \bar{f}_\theta\|^2}{trace(I - A_{(0)}(\theta))}$ and $\hat{\sigma}^2 = \frac{\|y - S\alpha - \bar{f}_\theta\|^2}{trace(I - A(\theta))}$ for the models (5) and (9) respectively. Luo et al. (1998) used a combination of subjective methods for (θ_1, θ_2) and GCV for (θ_3, θ_4) but the results here are similar.

3.4 Bayesian interpretation of the SS-ANOVA fit

It is well known (see, for example Kimeldorf & Wahba (1970), Wahba (1982*b*),Wahba (1983)), that there is a relationship between the solutions to variational problems of the form (6) and Bayes estimates, for particular given θ. This will provide the link between the spline ANOVA/partial spline models just described; the classical detection of signal in noise; and fingerprint methods. In our case the corresponding Bayes model for f is

$$f(t,P) = \sum_{k=1}^{p} \alpha_k S_k(t,P) + d_1 + d_2\phi(t) + Z(t,P), \quad t = 1,\cdots,n, \quad P \in \mathcal{S}, \tag{14}$$

where non-informative priors are attributed to the α's and d's and $Z(t,P)$ is a zero-mean Gaussian stochastic process with covariance

$$\frac{1}{\sigma^2} EZ(t,P)Z(t',P') = Q_\theta(t,P;t',P'), \tag{15}$$

where $Q_\theta(t,P;t'P')$ is given in (8). More details may be found in Wahba (1983), Wahba (1990). Then the minimizer f_θ of (6) evaluated at (t,P) is the conditional mean of $f(t,P)$ under the Bayes model (14),

$$f_\theta(t,P) = E[f(t,P)|y_1,\cdots,y_n], \quad t \in \{1,\cdots n_1\}, \quad P \in \mathcal{S}, \tag{16}$$

and the posterior covariances of f and its components, given the observations follows, see Wahba (1983), Gu & Wahba (1993) and below.

3.5 Fingerprinting

The previous results will now be related classical theory of the detection of signal in noise, and to fingerprinting. Think of as $S_1(t,P),...,S_p(t,P)$ as additive patterns induced by increases in greenhouse gas concentration, sulfate aerosol, solar cycle effect, or other human activities expected to impact the climate system. Information concerning the S_k's will come from climate model output. In the classical signal in noise model (with parametric signal), the observation vector y is modeled as

$$y = S\alpha + N_{\theta,\sigma} \tag{17}$$

where $N_{\theta,\sigma}$ is a vector representing natural climatic variability plus sub grid scale processes plus observational error, which may depend on some parameters (here θ,σ). Set $N_{\theta,\sigma} = \bar{f}_{\theta,\sigma} + \epsilon_\sigma$ where $\bar{f}_{\theta,\sigma}$ is an n vector with ith entry $f_{\theta,\sigma}(t_i,P_i)$. Here $f_{\theta,\sigma}(t,P)$ represents natural climate variability[8], and $\epsilon_\sigma = (\epsilon_1,\cdots,\epsilon_n)'$ is a vector representing subgrid scale and observational noise, which will be modeled as independent, identically distributed zero mean Gaussian random variables with common variance σ^2. Assuming $N_{\theta,\sigma}$ is modeled as a zero

[8]Here σ^2 enters as a parameter in $f_{\theta,\sigma}$ because the θ are actually signal to noise rations rather than signal intensities, due to the appearance of σ^2 on the left hand side of (15)

mean random vector with covariance $C_{\theta,\sigma}$, then the minimum variance unbiased estimate $\hat{\alpha}$ of α is

$$\hat{\alpha} = (S'C_{\theta,\sigma}^{-1}S)^{-1}S'C_{\theta,\sigma}^{-1}y. \tag{18}$$

Statistical inference can be based on the fact that, under Gaussian assumptions on $f_{\theta,\sigma}$ and ϵ_σ, $\hat{\alpha}$ has a multivariate normal distribution:

$$\hat{\alpha} \sim N(\alpha, (S'C_{\theta,\sigma}^{-1}S)^{-1}), \tag{19}$$

see Rao (1973). It can be shown that $\hat{\alpha}$ produced in the minimization of (10) produces the $\hat{\alpha}$ of (18), where $C_{\theta,\sigma}^{-1}$ is the inverse covariance matrix of $N_{\theta,\sigma}$ implied by the Bayes model with $f(t,P)$ in (10) assigned the distributions given in (14) and(15) for $f_{\theta,\sigma}$[9].

A formal test of the no signal hypothesis may be written as

$$H_0 : \ \alpha = 0 \quad vs. \quad H_1 : \ \alpha \neq 0. \tag{20}$$

If $C_{\theta,\sigma}$ is known, then the hypothesis test of (20) rejects H_0 if

$$\begin{aligned} T^2 &= \hat{\alpha}'(S'C_{\theta,\sigma}^{-1}S)\hat{\alpha} \\ &> \mathcal{X}_p^2(\delta), \end{aligned} \tag{21}$$

where $\mathcal{X}_p^2(\delta)$ is the upper (100δ)th percentile of the chi-square distribution with p degrees of freedom. Many, if not most of the fingerprinting methods being applied are based on this hypothesis testing paradigm, see, for example Hegerl & North (1997).

Disregarding for the moment the preceeding theoretical results, the hypothesis tests here will primarily be based on reference distributions obtained from forced and background climate runs with added realistic sub grid scale noise. To study the variability of $\hat{\alpha}$ under the null and specific alternative hypotheses, simulated noisy observations were produced at the observation points by carrying climate model output to the observation points (t_i, P_i) and adding subgrid scale noise with realistic variance, to produce replicates of simulated y vectors, with and without signal. These simulated data vectors were then analyzed in the same manner as the historical data vector, to obtain empirical reference distributions for the test statistics. The test statistics based on historical data are then compared to the reference distributions.

There are several theoretical and empirical results, generally in simpler contexts than that involved here, which indicate that posterior variances obtained from implied covariance matrices analogous to the one in (19) tuned by generalized cross validation can provide good estimates of the variance of the test statistics. See Wahba (1983), Nychka (1988), Nychka (1990), Gu & Wahba (1993). Therefore it was decided to compare the reference distributions based on climate model background runs with the distribution in (19), to assess to what extent the use of (19) may be reasonable.

[9]Since d_1 and d_2 have improper priors, $C_{\theta,\sigma}$ strictly speaking has components which are not finite, but $C_{\theta,\sigma}^{-1}$ is well defined, see Wahba (1990)

4 The experiments

4.1 Experiment 1. single signal

In the first experiment a single signal, $p = 1$ was considered. It was taken as the linear component of the time trend of the spatial anomaly due to forcing. Thus, $S(t, P) = f_{\phi,2}(P)\phi(t)$, where $f_{\phi,2}$ is obtained from ANOVA decompositions of the form (2). First the five 30 year forced runs from GFDL and NCAR1, ..., NCAR4 were quasi-interpolated to the observational data points, and the ANOVA decomposition (2) obtained via the algorithm in Luo et al. (1998) and Luo (1998), with θ computed for climate model output as described in Appendix A. Similarly the corresponding background runs are decomposed and the background $f_{\phi,2}(P)\phi(t)$ was subtracted from the forced $f_{\phi,2}(P)\phi(t)$ at the observation points in each of the five cases to obtain the five signals due to forcing, which are n-vectors, labeled here $S_{GFDL}, S_{NCAR1}, \cdots S_{NCAR4}$.

To obtain reference distributions for $\hat{\alpha}$ under the null hypothesis, 29 disjoint 30-year pieces of the GFDL 1000 year background run (not including the 30-year piece that corresponds to the forced run) were used as proxies for natural variability. Let h_j be the $n = 23$ 119-vector of the jth 30-year piece carried over to the observation points as in Appendix A. The h_j were treated as though they were random vectors independent of one another. Of course they are neither random nor independent but we believe this to be a useful fiction. Twenty nine simulated background climate data sets $u_1, \cdots, u_{29}$ were obtained as $u_j = h_j + e_j$, where e_j was a vector of n independent, zero mean Gaussian pseudo-random numbers with standard deviation $\sigma = .4755$. This value of σ was obtained from the (GCV-based) estimate of σ from a decomposition of the historical data of the form (2). Other authors have reported similar values for the subgrid scale standard deviation of surface temperature data, see for example Jones (1994). GCV estimates of θ were obtained for the first run, and the same θ were used for all twenty-nine runs. It was expected based some preliminary experimentation that the θ would change very little from run to run. Next, 29 proxies for forced data sets with $\alpha = 1$ were generated by adding a term due to forcing to the simulated observational data. The simulated forced runs $u_j, j = 1, \cdots 29$ were obtained as $u_j = [GFDL\ forced - GFDL\ background] + h_j + \epsilon_j$ where $[GFDL\ forced - GFDL\ background]$ is the difference of the indicated climate runs, after being carried over to the n observation points. $GFDL\ background$ is the 30 year background run for the same time period as $GFDL\ forced$. The resulting estimates of α's and their corresponding d_2 are given in Figure 15.

Note that d_2 is the coefficient of overall linear trend and α is the coefficient of S_{GFDL} representing the space-varying signal coefficient. Figure 15 panel (a) gives histograms of the 29 estimates of α, for the 29 forced simulated data sets and the 29 background simulated data sets. Panel (b) gives histograms of the estimates of d_2, and panel (c) gives a scatter plot of the (d_2, α) pairs, along with a '*' for the (d_2, α) pair estimated from the historical data. It can be seen that the forced and background distributions of the α estimates are well separated, providing the *potential* for relatively strong attribution conclusions, while the d_2 distributions are not so well separated. Analysis of the historical data resulted in an observed estimate of d_2 equal to 0.01632^oC/yr, which was close to the average of the forced proxy estimates, which was 0.01751. However, the estimate of α from the historical

data, which was -0.06885, was quite different from the forced proxy estimate. This result suggests that the GFDL model output is close to the historical time trend on a very large spatial scale, but not on the scale of the spatial anomaly anywhere near the level of detail that is incorporated in our signal here. It is fairly clear that the more complex the signal, the greater the separation it potentially provides between forced and background climate statistics. However, as we shall see by example, it also puts greater demands on the model for a more accurate signal. A simple mathematical formalism illustrating this argument is in Section 5. Other authors have made similar remarks, see, for example Santer, Cubasch, Mikolajewicz & Hegerl (1993), Barnett et al. (1998), Hegerl & North (1997).

Similar results were obtained for the four NCAR signals using $[NCAR\,forced - NCAR\,background]$ for the term due to forcing, although it was necessary to use the 29 GFDL background backgrounds (h_j) as proxies for the natural variability, since long NCAR background runs were not available to us at the start of this study. The results are given in Table 1 and, for NCAR1 in panels (d), (e) and (f) of Figure 15. The systematic bias in $\hat{\alpha}$ for the forced runs (the true α is 1), is believed to be at least partly related to the manner in which the simulated forced runs were generated. The $[forced - background]$ component not along the signal direction appeared in each of the 29 runs and appeared as a common background component.

Table 1: Sample means and standard deviations of 29 estimates of α from the five sets of forced and background proxies.

Signal	Runs	Sample Mean	Sample Std Dev
GFDL	Background	0.018144	0.081337
	Forced	0.947155	0.079970
NCAR1	Background	0.015360	0.046893
	Forced	0.844409	0.044854
NCAR2	Background	-0.005143	0.056953
	Forced	0.791295	0.056305
NCAR3	Background	-0.002736	0.064896
	Forced	0.815897	0.064621
NCAR4	Background	-0.018810	0.067442
	Forced	0.835242	0.071268

The historical data is searched using each of the five signals described above. In all five cases, the estimated α was well within the interior of the no signal distribution of α. The d_2, α pairs are given in Table 2.

4.2 Experiment 2. composite signal

Instead of a single signal, a composite signal was formed as a linear combination of the NCAR1 and NCAR2 signals to test the ability of the method to extract a signal of this form. The signal was formed as $\alpha_1 S_{NCAR1} + \alpha_2 S_{NCAR2}$, where $\alpha_1 + \alpha_2 = 1$.

Twenty-nine sets of simulated observations were generated as before with the composite

Table 2: Estimates of α and d_2 from the historical data.

Signal	$\hat{\alpha}$	$\hat{d_2}$
GFDL	-0.068850	0.016322
NCAR1	-0.052302	0.015985
NCAR2	0.006250	0.015748
NCAR3	-0.102460	0.016020
NCAR4	-0.148983	0.015600

signal:

$$u_j = \alpha_1[NCAR1\ forced] + \alpha_2[NCAR2\ forced] - [NCAR\ background] + h_j + e_j, \quad (22)$$

with $\alpha_1 + \alpha_2 = 1$, $j = 1, ..., 29$. For each data set, a partial spline model (9) was fitted by minimizing (10). Histograms of the resulting α_1 and α_2 estimates were obtained. The previous set of 29 proxies for background data sets that were used to obtain null reference distributions in Section 4.1 were also analyzed for α_1 and α_2. The histograms under the null and under the alternative were very well separated. The results are plotted in Figure 16, panels (a), (b) and (c), where the simulated $(\alpha_1, \alpha_2) = (0.65, 0.35)$. Table 3 summarizes the sample means and standard deviations. Similar results were obtained with other values of (α_1, α_2).

Table 3: Sample means and covariance matrices of estimates of α from forced and background proxies, composite signal case.

	Sample Mean	Sample Covariance
Background	(-0.002356,0.025392)	[0.003704,-0.003077] [-0.003077,0.005636]
Forced $(\alpha_1, \alpha_2) = (0.65, 0.35)$	(0.563692,0.255347)	[0.003950,-0.003342] [-0.003342,0.005879]

This suggests that if the forcing is representable as some (unknown) linear combination of signals, then there is the potential for estimating the mixture and using the results in a test. Other authors have considered multiple signals, included solar and volcanic forcing in greenhouse studies. See, for example North & Stevens (1998*a*), also Hasselmann (1998). In particular, an event of the magnitude of Pinatubo would probably adversely affect the linear trend component if not accounted for.

The historical data was tested for the presence of a signal of the form $\alpha_1 S_{NCAR1} + \alpha_2 S_{NCAR2}$. However some mixture of these two signals was not detected above the background natural variability, the estimated historical (α_1, α_2) was $(-0.096466, 0.072024)$.

4.3 Experiment 3. analysis with an erroneous signal

To try to get some idea of the requirements on signal accuracy when using $S(t, P) = f_{\phi,2}(P)\phi(t)$ as the signal, the 29 proxy data sets forced with the GFDL signal as in Section 4.1, were analyzed using the NCAR1 signal.

It was found that when the 29 forced data sets containing the GFDL signal were analyzed using S_{NCAR1}, all but about five of the replicates had their estimated α down in the background α distribution. Hence, if the 'true' 1% CO_2 linear component of the time trend of the spatial anomaly in the historical data were much like the GFDL signal, but the historical data were analyzed based on the NCAR1 signal, detection would be moderately unlikely, even though detection and attribution of a signal known very accurately would be highly likely. Figure 17 and Table 4 summarize the result. The background distribution of the α estimates is the same as that in the $NCAR1$ Background row of Table 1.

Table 4: Sample means and standard deviations of estimates of α from forced and background proxies, erroneous signal case.

	Sample Mean	Sample Std Dev
Background	0.015360	0.046893
Forced	0.146475	0.048926

This says that for this signal, the linear component of the time trend spatial anomaly, to be practically useful for detection and attribution, it will be necessary to know it with more accuracy than the difference between the GFDL and the NCAR1 1% (CO_2) runs. This appears to be a rather negative result, but it is necessary to keep in mind the quite fine level of detail of the signal being studied. Further comments concerning signal selection are made in Section 5.

4.4 Bayes parameters

It is well-recognized in the climate change literature that the estimation of the covariance matrix $C_{\theta,\sigma}$ is a difficult task regardless of one's view of the detection-attribution problems. In this experiment, it is examined whether using the Bayesian interpretation of the solution to the variational problems (6) and (10) with the GCV estimate of the parameters (θ, σ) results in realistic estimates for the distribution of $\hat{\alpha}$ in the present context. Theoretical results in simpler contexts suggest that this is a reasonable question, see Wahba (1983), Nychka (1988), Nychka (1990), Gu & Wahba (1993). By substituting (13) into (12), it can be seen that $\hat{\alpha}$ can be estimated via backfitting as

$$\hat{\alpha} = (S'(I - A_{(0)}(\theta))S)^{-1}S'(I - A_{(0)}(\theta))y, \tag{23}$$

where $A_{(0)}(\theta)$ is the influence matrix provided $\alpha = 0$ in the partial spline model. After some algebra, the theoretical distribution of the estimate of α, assuming the Bayes model (14), can be obtained as

$$\hat{\alpha} \sim N(\alpha, \sigma^2(S'(I - A_{(0)}(\theta))S)^{-1}). \tag{24}$$

Comparing (19) and (24) we find that $\sigma^2 C_{\theta,\sigma}^{-1} = (I - A_{(0)}(\theta))$. Hence the parameters embedded in the implicit covariance matrix for the natural variability are being directly estimated from the data set being analyzed based on GCV. The Bayesian estimates of standard deviation (Experiments 1 and 3) and covariance matrix (Experiment 2) based on (24) are given

in Table 5. Note that $A_{(0)}(\theta)S$ can be computed by giving the LW algorithm the columns of S as 'data'. Comparing Tables 5 and 1 it is seen that the Bayesian standard deviations for the GFDL forced and background distributions are very close to the standard deviations based on 29 segments of the GFDL climate background run, while the NCAR Bayesian standard deviations are systematically smaller than their counterparts from the climate model reference distributions, which are themselves smaller than the GFDL reference standard deviations. This experiment also provided a chance to examine the estimates of σ, the standard deviation of the ϵ_i, which were simulated with the standard deviation $\sigma = .4755$, the historical estimate. (The estimates and not the true value were used in computing the entries in Table 5). The σ estimates for the GFDL Background and Forced runs were .44 and .42 respectively and .43 and .41 for the four NCAR Background runs and the four NCAR Forced runs respectively, about a systematic 10% underestimate.

Table 5: Bayesian standard deviation and covariance estimaes for Experiments 1,2, and 3.

Corresp. Experiment	Run	Standard Deviation
Experiment 1 GFDL	Background	0.083117
	Forced	0.078358
Experiment 1 NCAR1	Background	0.034204
	Forced	0.037350
Experiment 1 NCAR2	Background	0.035579
	Forced	0.038933
Experiment 1 NCAR3	Background	0.038064
	Forced	0.041379
Experiment 1 NCAR4	Background	0.038614
	Forced	0.042108
Experiment 3	Background	0.034204
	Forced	0.041274
Corresp. Experiment	**Run**	**Covariance**
Experiment 2	Background	[0.002016,-0.001334]
(α_1,α_2)=(0.65,0.35)		[-0.001334,0.002172]
	Forced	[0.002297,-0.001518]
		[-0.001518,0.002484]

One limitation of the study here is that only the long GFDL background run was available to create backgrounds, and so the GFDL background runs were used with both GFDL signals and the NCAR signals. We believe that using GFDL background with an NCAR signal is likely to be the reason why the NCAR Bayes standard deviation for $\hat{\alpha}$ did not match the NCAR reference standard deviation as well as the GFDL Bayes standard deviation matched the GFDL reference standard deviation. If the GFDL signal with GFDL background comparison provides the more realistic comparison, this could be attributed to be a result of the GCV estimation estimation of the θ, σ from the data. These parameters capture the most important tuning parameters in $C_{\theta,\sigma}$. This would support the proposition that it is only necessary to fit a few of the most important parameters in covariance models when

using them as they are being used here. This will be discussed further in Section 6.1. We do not know at this point whether more general conclusions from the GFDL experimental result can be drawn, but if there are any to be drawn, it is that there is the potential for estimating certain of the most important parameters in the required covariances (penalty functionals) simultaneously with the signal intensities, directly from the historical data sets being analyzed.

5 Tradeoffs in signal selection

There are many tradeoffs in the choice of signal, or fingerprint, certainly tradeoffs between utilizing the various kinds of observational data with their systematic and non-systematic errors. Other things being held fixed for expository purposes here a tradeoff between signal specificity or complexity and model is examined. Suppose the data is analyzed using S, the climate model output for signal, but the 'true' signal is actually $S + \Delta$. Then the estimate $\hat{\alpha}$ will be biased,

$$E(\hat{\alpha} - \alpha) = (S'C^{-1}S)^{-1}S'C^{-1}\Delta\alpha, \tag{25}$$

where the θ, σ is suppressed, to emphasize the generality of this argument. The bias can, hopefully, be reduced as follows. Let F be a $q \times n$ matrix chosen so that $F\Delta$ is believed to be small (ideally 0). For example, if Δ is a 'high frequency' error then F could be a filter which damps out the high frequencies. Now consider the corresponding projected model

$$\tilde{y} \equiv Fy = FS\alpha + FN \equiv \tilde{S}\alpha + \tilde{N}. \tag{26}$$

Then the covariance of $\tilde{N}$ is $\tilde{C} = FCF'$, say[10], and the estimate $\hat{\alpha_F}$ of α is

$$\hat{\alpha_F} = (\tilde{S}'\tilde{C}^{-1}\tilde{S})^{-1}\tilde{S}'\tilde{C}^{-1}\tilde{y}. \tag{27}$$

The covariance of $\hat{\alpha}$ is $(S'C^{-1}S)^{-1}$, which may be compared to the covariance of $\hat{\alpha_F}$, which is $(\tilde{S}'\tilde{C}^{-1}\tilde{S})^{-1}$. It can be shown that for any p-vector x, $x'(\tilde{S}'\tilde{C}^{-1}\tilde{S})^{-1}x \geq x'(S'C^{-1}S)^{-1}x$ [11], so that the variance of any linear combination of the components is only increased by projecting the observations via F, while the bias is decreased.

Considering the decomposition (2), it is much easier for a climate model to generate an accurate d_2 than an accurate $f_{\phi,2}(P)$. With observations scattered in time and space it may be more intuitive to consider obtaining a less complex signal from a more complex signal $S(t, P)$ by smoothing or filtering $S(t, P)$ in the tensor product domain in t and P. For example one could consider

$$\tilde{S}(t, P) = \int_S F(P, P')f_{\phi,2}(P')\phi(t)dP', \tag{28}$$

where $f_{\phi,2}$ was obtained from climate model output as in Section 4 for appropriate $F(P, P')$.

[10] For arguments sake we are assuming that C is reasonably correct here.

[11] To see this we need to show that $(S'F'(FCF')^{-1}FS) \succeq (S'C^{-1}S)^{-1}$, equivalently $S'C^{-1}S \preceq S'F'(FCF')^{-1}FS$, equivalently $C^{-1} \preceq F'(FCF')^{-1}F$, equivalently $I \preceq C^{1/2}F'(FCF')^{-1}FC^{1/2}$, where $A \succeq B$ means that $A - B$ is positive definite, and $C^{1/2}$ is the symmetric square root of C. The result follows by substituting in the singular value decomposition for $FC^{1/2}$.

6 Generalizations

6.1 Other covariances

The ANOVA decomposition (2) is well defined for any function $f(t,P)$ $t \in 1,2,\cdots,n_1, P \in \mathcal{S}$ independent of any choice of penalty functional, (equivalently, any covariance). The models here are built up from tensor products of time and space models, which admit of a variety of generalizations. However, the tensor product structure makes it easy to compute the anomalies, as well as to carry out the backfitting via the LW algorithm. Second difference and Laplacian penalties and their associated reproducing kernels (covariances) were chosen because they are fairly robust general purpose smoothers or low pass filters. Only a few free parameters (θ,σ) are considered, partly because of the limitations of fitting models with more parameters given the scattering of the observations in time and space, and partly the lack of obvious physical reasons for choosing other particular models, although such may exist. It is straightforward to replace the covariance associated with J_2 with other covariances on the sphere, if warranted. $J_1(f_1)$ may be replaced, for example, by the third difference: $\sum_{t=1}^{n_1-3}(f(t+3)-3f(t+2)+3f(t+1)-f(t))^2$. Then L in Appendix A.1 becomes the analogous $n_1 \times (n_1-3)$ matrix with first row $(1,-3,3,-1,0,\cdots 0)$. J_1 then has two unpenalized vectors (in addition to the constant vector), namely, $\phi_1 = \phi$, and ϕ_2 where $\phi_2(t)$ is quadratic in t and orthogonal to the constant vector and to ϕ_1. There will be more terms in the ANOVA decomposition, including the quadratic component of the time trend. Penalties of the form $J_1(f) = \sum(f(t+1) - af(t))^2$ and higher order generalizations can also be used. The trend terms will then be vectors which are in the null space of J_1.

A general class of stochastic models discrete in time and continuous in space (on the sphere) may be described as

$$X(t,P) = \sum_{\mu,\nu} z_{\mu,\nu}(t)\lambda_{\mu,\nu}^{1/2}\Psi_{\mu,\nu}(P) \tag{29}$$

where the $z_{\mu,\nu}$ may be fixed functions, may satisfy difference equations driven by discrete white noise, the $z_{\mu,\nu}$ may be independent or not, they may be chosen for simplicity, fitted to data or model output, or derived from some physical principles, and the $\Psi_{\mu,\nu}$ may be spherical harmonics, eigenfunctions of some differential operator relevant to the problem at hand, empirical orthogonal functions or mixtures of these. Alternatively X may be the solution of some partial difference-differential equation driven by some stochastic process, see Bennett (1997), Wahba (1998). A short list of papers involving various kinds of time and space models would include Kaplan, Kushnir, Cane & Blumenthal (1997), Kaplan, Cane, Kushnir, Clement, Blumenthal & Rajagopalan (1998), Polyak (1996), North & Stevens (1998*b*), Bloomfield & Nychka (1992), Kooperberg & O'Sullivan (1996), North & Stevens (1998*b*), North & Stevens (1998*a*), Polyak (1996).

To be useful, of course, appropriate computable expressions for the covariances must be available. A variety of special cases can be fitted via the LW algorithm. The model used here is equivalent to

$$X(t,P) = \sum_{\mu=-1}^{1}\sum_{\nu=0}^{\infty} z_{\mu,\nu}(t)\lambda_{\nu}^{1/2}\Psi_{\nu}(P), \quad \lambda_0 = 1, \quad \Psi_0(P) = 1, \tag{30}$$

where $\sum_{\nu=1}^{\infty} \lambda_\nu \Psi_\nu(P)\Psi_\nu(Q) = R_s(P,Q)$, with $R_s(P,Q)$ given in Appendix A.1. The $z_{\mu,\nu}(\cdot)$ vectors are independent for $\mu,\nu \neq \mu'\nu'$, and

$$\begin{array}{llllll} z_{-1,0}(t) & = & d_1; & z_{-1,\nu}(t) & = & z_{-1,\nu} \quad \sim \mathcal{N}(0,\theta_2), \quad \nu = 1,2,\cdots \\ z_{0,0}(t) & = & d_2\phi(t); & z_{0,\nu}(t) & = & z_{0,\nu} \quad \sim \mathcal{N}(0,\theta_3), \quad \nu = 1,2,\cdots \\ z_{1,0}(t) & \sim & \mathcal{N}(0,\theta_1 R_t(t,\tau)); & z_{1,\nu}(t) & \sim & \mathcal{N}(0,\theta_4 R_t(t,\tau)), \quad \nu = 1,2,\cdots, \end{array}$$

the univariate random variables d_1 and d_2 have diffuse priors, and the $n_1 \times n_1$ covariance matrix $R_t(t,\tau)$ for the random vector $z_{1,0}(\cdot)$ is given in Appendix A.1.

To use the methods here, a small set of the most important and relatively unaliased free parameters (here θ, σ) must be isolated and the models tuned appropriately. Maximum likelihood estimates of certain parameters may also be considered, see Dee, Gaspari, Redder, Rukhovets & daSilva (1998). However, we believe that that our present conclusions are relatively robust to reasonable changes in the model used here.

6.2 Three space dimensions

A vertical coordinate may be included, which may be discrete or continuous, depending on the application. Santer et al. (1996), Tett et al. (1996) and others have considered the vertical temperature distribution. Letting z be a (continuous) vertical coordinate, mapped into $[0,1]$ (not to be confused with the random variables in the preceding section). It is necessary to define a vertical averaging operator, for example

$$\mathcal{E}_z f(t,P,z) = \int_0^1 f(t,P,z)dz. \tag{31}$$

Then, analogous to (1) there is decomposition of the identity:

$$I = (\mathcal{E}_t + (I-\mathcal{E}_t))(\mathcal{E}_P + (I-\mathcal{E}_P))(\mathcal{E}_z + (I-\mathcal{E}_z)) \tag{32}$$

which can be expanded as before, to obtain the anomalies of interest. A commonly used penalty functional is $\int_0^1 (f''(z))^2 dz$, see Wahba (1990) for a reproducing kernel associated with this penalty functional, details are omitted. Examples of ANOVA decompositions of several variables in a different context may be found in Wahba et al. (1995).

6.3 Indirect observations

The analysis so far considered only direct observations (a.k.a.'point evaluations') that is, direct observations of $f(t_i,P_i)$, or, if a vertical dimension is included, $f(t_i,P_i,z_i)$. Considering a three dimensional analysis, and linearizing (a matter which has to be justified or accounted for), suppose indirect (satellite) radiance information which may be (approximately!) described in the form

$$y_i^s = \int_{surface}^{top} K_i(P_i,z) f((t_i,P_i,z)dz + \epsilon_i \equiv L_i(f) + \epsilon_i, \quad [say], \tag{33}$$

is available, where K_i (which is assumed here to be invariant over time) is known. The superscript s has been inserted to indicate satellite information. Then a term of the form

$$\sum_{i,j} w_{ij}(y_i^s - L_i(f))(y_j^s - L_j(f)) \tag{34}$$

can be added to the variational problems (6) or (10). Here the w_{ij} represent a quadratic form which should encode the covariance (scaled relative to the errors of other observations) of the ϵ_i which now may not be independent. In practice, L_i might most conveniently represent a (carefully chosen) linear combination of raw observations ('superob'). The (exact) solutions of the minimization problems then include basis functions which are the representers of the L_i. They are functions of the form $\eta_i(t,P,z) = L_{i(t',P',z')}(t,P,z)Q_\theta(t',P',z';t,P,z)$, where $L_{i(t',P',z')}$ means the linear functional L_i applied to what follows, considered as a function of (t',P',z'). See Kimeldorf & Wahba (1971), Wahba (1990) Section 1.3, O'Sullivan & Wahba (1985), Bennett (1992). In practice approximate methods will no doubt be necessary.

6.4 Other applications

The ANOVA decomposition and signal detection approach here has potential for use in other applications. For example, consider a forecast model, where observations minus forecast (O-F) are available in observation space, for a series of successive time periods. The methods here may be used to look for possibly spatially dependent biases, trends or drifts by examining the various anomalies. If a systematic model error may be obtained as an approximately additive signal, by for example, looking at the difference between forecasts after perturbing some quantity in the model that is suspect of being in error, then this 'signal' may possibly be searched for in the O-F data sets by the methods described here.

7 Conclusions

Smoothing spline ANOVA and partial spline methods provide a flexible family of methods for examining fingerprints in observation space, and to compare historical data and climate model output from different models. They allow the analysis to be carried out in observation space, thus reducing the errors and assumptions made when carrying scattered historical data to climate model output coordinates. Mixtures of signals can be handled by the proposed methods.

It is shown via a set of experiments that this class of methods has the potential for high-powered signal detection, but to reap these benefits, a higher degree of accuracy of climate model output is required than was available for this study.

There is some evidence that a small number of parameters in (prior) covariances can be estimated simultaneously with signal statistics from historical data. Further work is necessary here, but it may be possible to reduce somewhat the reliance on extensive background runs, or at least provide corroborating information, directly from historical data.

The class of methods generalizes to include vertical information, and to include indirect as well as direct observations.

A tradeoff needs to be be made between choosing a 'simple' signal with few degrees of freedom (broad averages, generally) which climate models can be expected to produce accurately as a result of greenhouse forcing, but which are harder to separate from 'background', and more detailed or complex signals, which are easier to separate cleanly from background, but harder to generate realistically. It is clear that improved climate models are of extreme importance, and further work is required to understand how to optimize this tradeoff, given a particular climate model.

8 Acknowledgments

We thank Jerry Meehl for providing the NCAR climate model output. This work was supported by NASA Grants NAG5 3769 and NAG5 4398; NSF Grants DMS9121003, DMS9704758 and DMS93122686 (under the Geophysical Statistics Project), and DOE Grant DE-FG02-92ER61439.

List of Figures

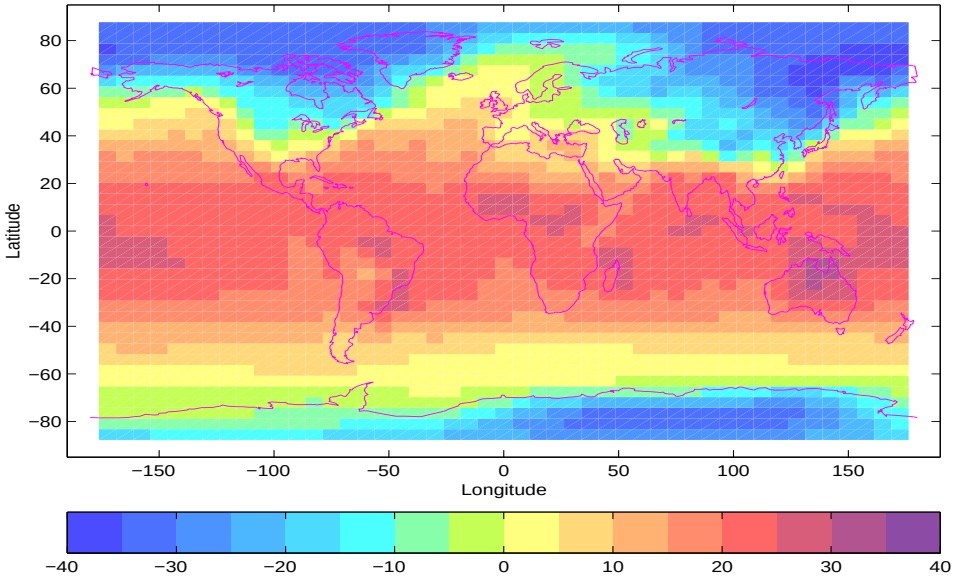

Figure 1: Mean of the GFDL forced run average winter temperature (^{o}C), 1961-1990, 1920 grid points.

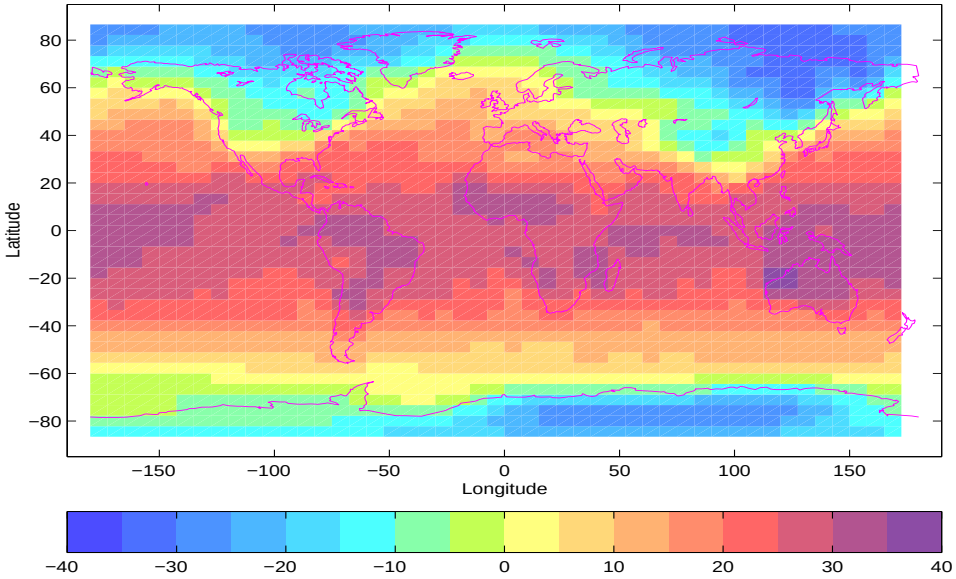

Figure 2: Mean of the NCAR1 forced run average winter temperature (^{o}C), 1961-1990, 1920 grid points.

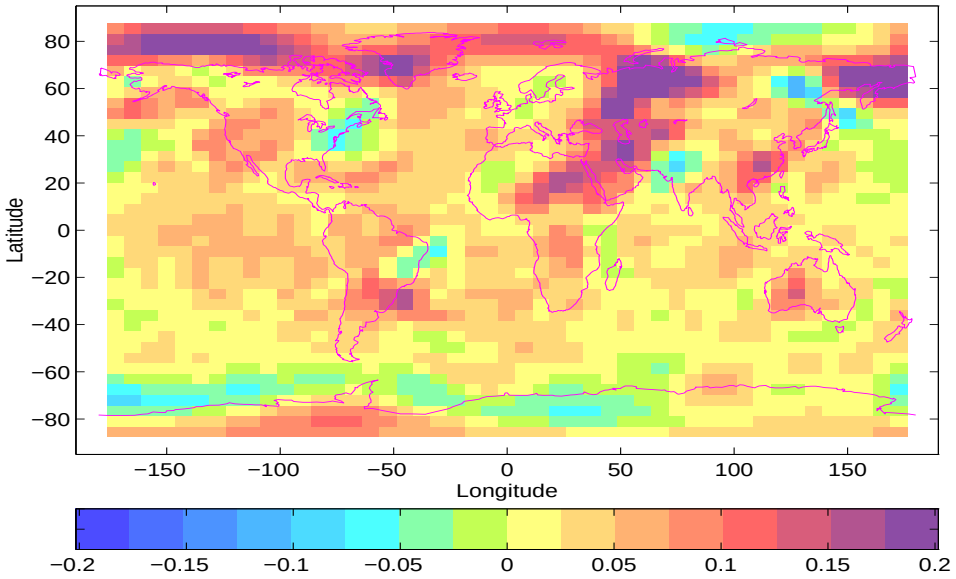

Figure 3: Linear trend of the GFDL forced minus background average winter temperature (^{o}C/yr), 1961-1990, 1920 grid points.

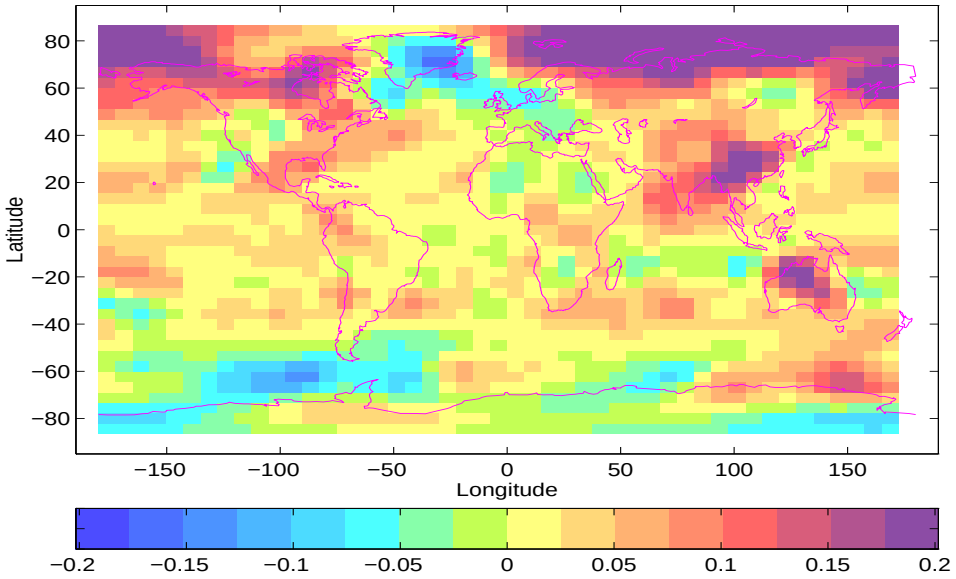

Figure 4: Linear trend of the NCAR1 forced minus background average winter temperature (^{o}C/yr), 1961-1990, 1920 grid points.

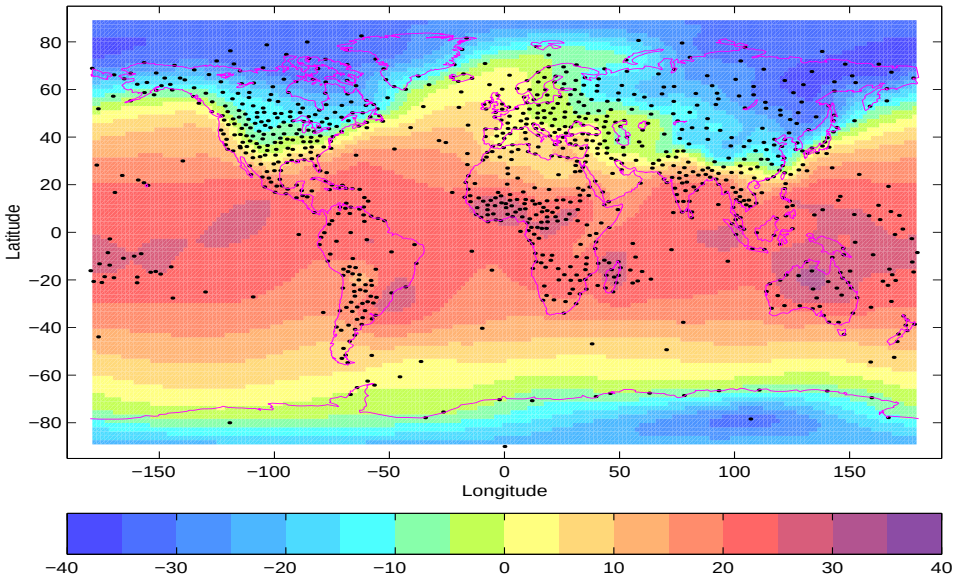

Figure 5: Mean of the GFDL forced run average winter temperature (^{o}C), 1961-1990.

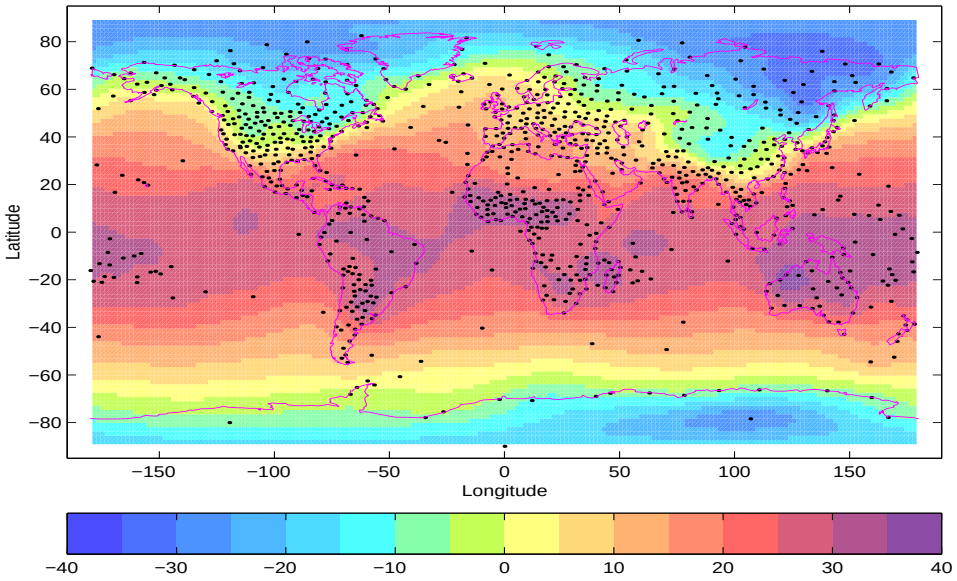

Figure 6: Mean of the NCAR1 forced run average winter temperature (^{o}C), 1961-1990.

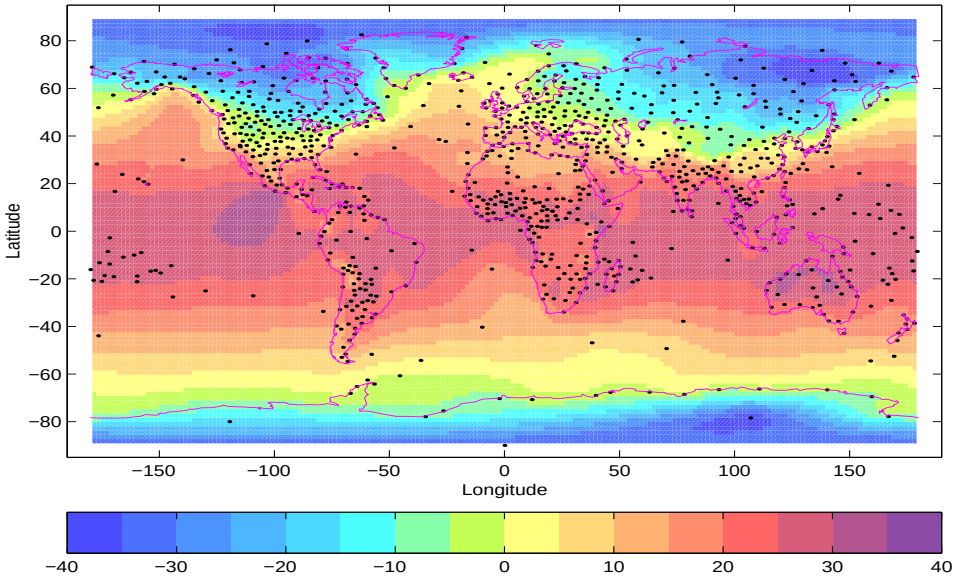

Figure 7: Mean of the historical average winter temperature (^{o}C), 1961-1990.

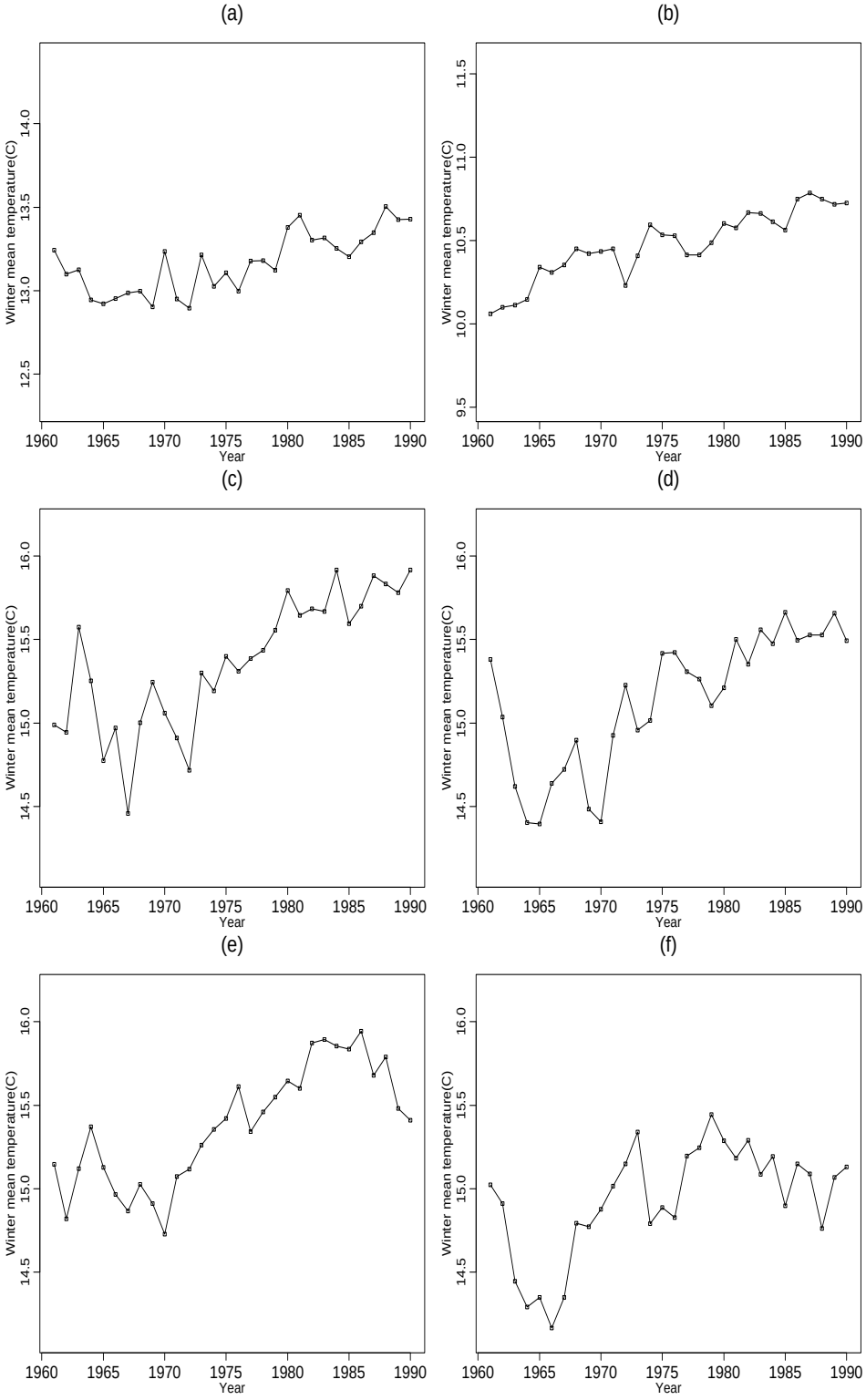

Figure 8: Yearly average winter temperatures (^{o}C): (a) Historical (b) GFDL forced (c) NCAR1 forced (d) NCAR2 forced (e) NCAR3 forced (f) NCAR4 forced.

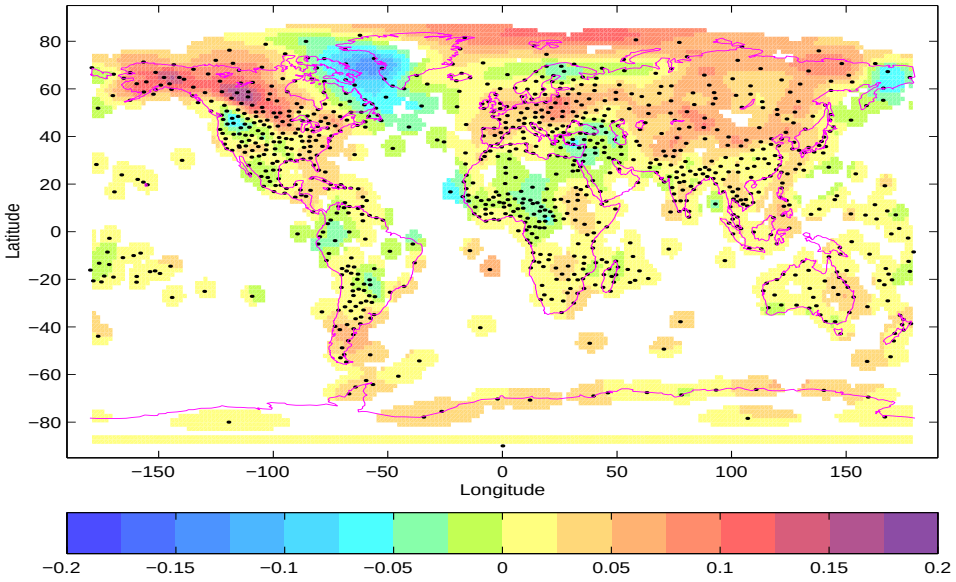

Figure 9: Linear trend of the historical average winter temperature (^{o}C/yr), 1961-1990.

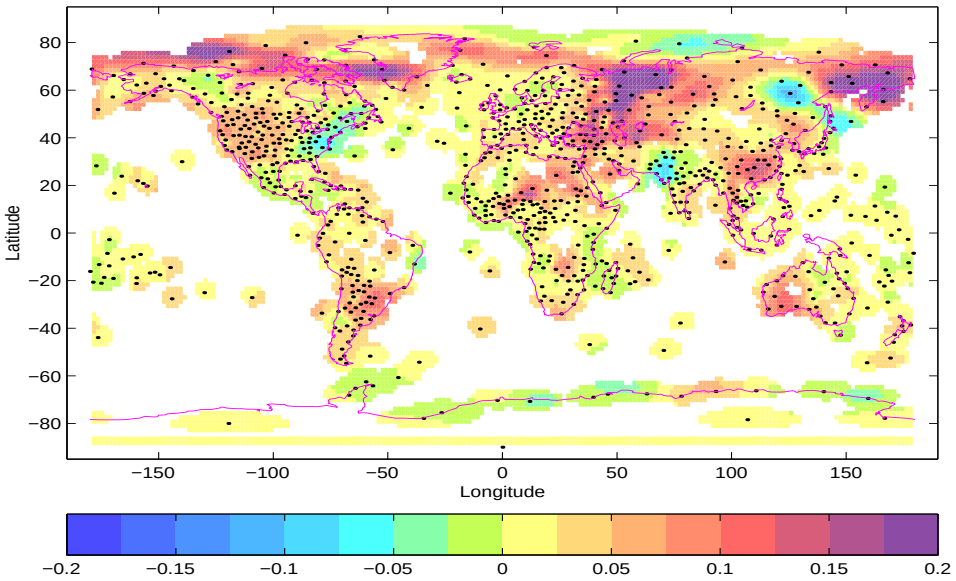

Figure 10: Linear trend of the GFDL forced minus background average winter temperature (^{o}C/yr),1961-1990.

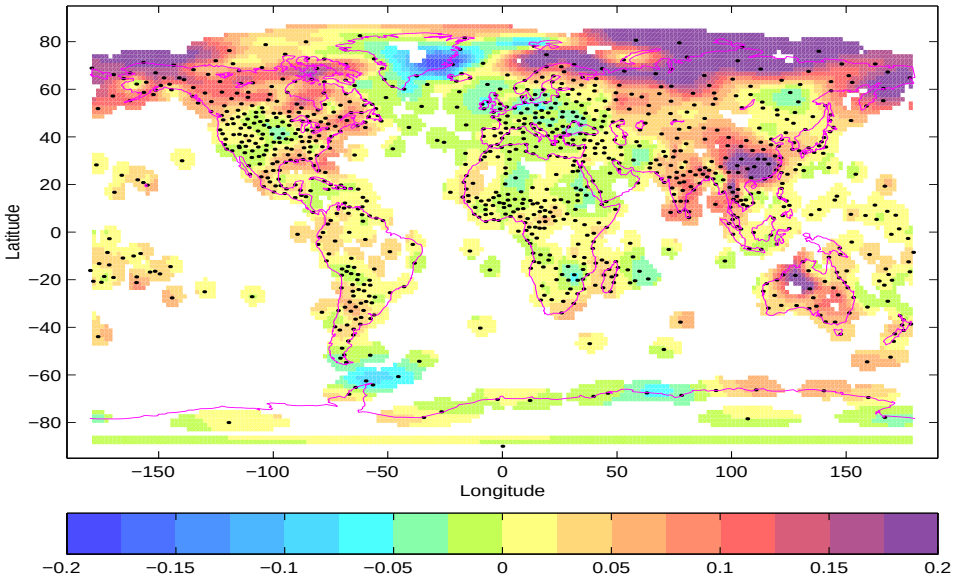

Figure 11: Linear trend of the NCAR1 forced minus background average winter temperature (^{o}C) in 1961-1990.

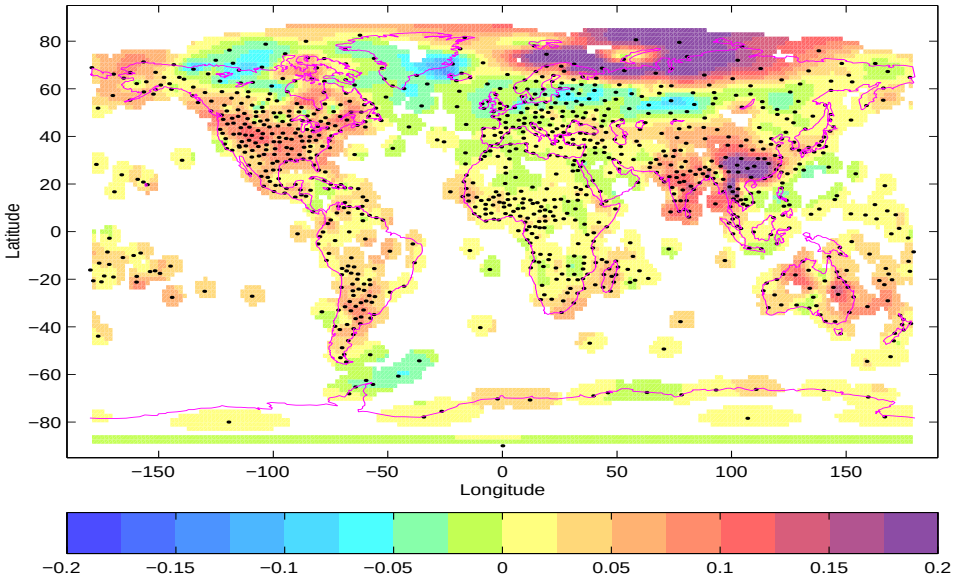

Figure 12: Linear trend of the NCAR2 forced minus background average winter temperature (^{o}C), 1961-1990.

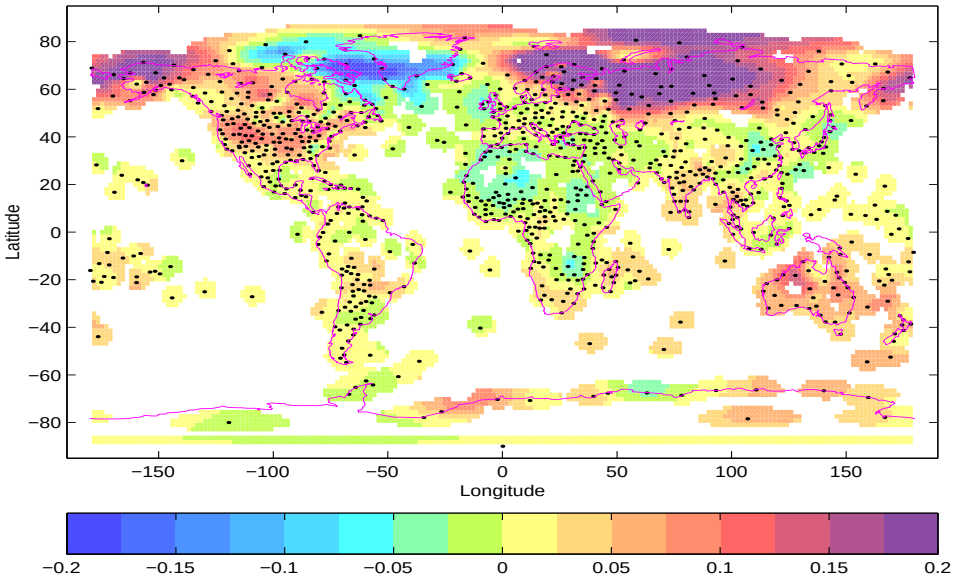

Figure 13: Linear trend of the NCAR3 forced minus background average winter temperature (^{o}C), 1961-1990.

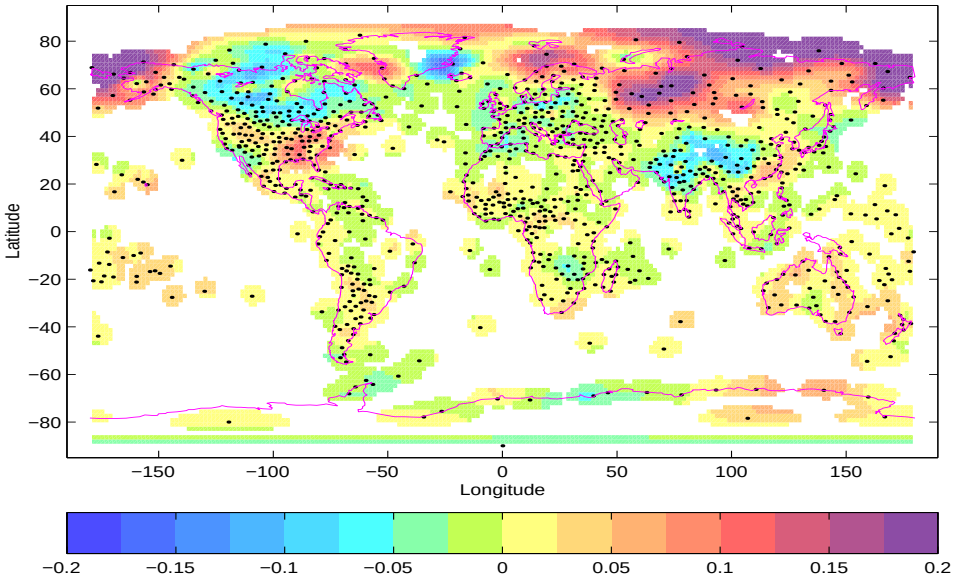

Figure 14: Linear trend of the NCAR4 forced minus background average winter temperature (^{o}C), 1961-1990.

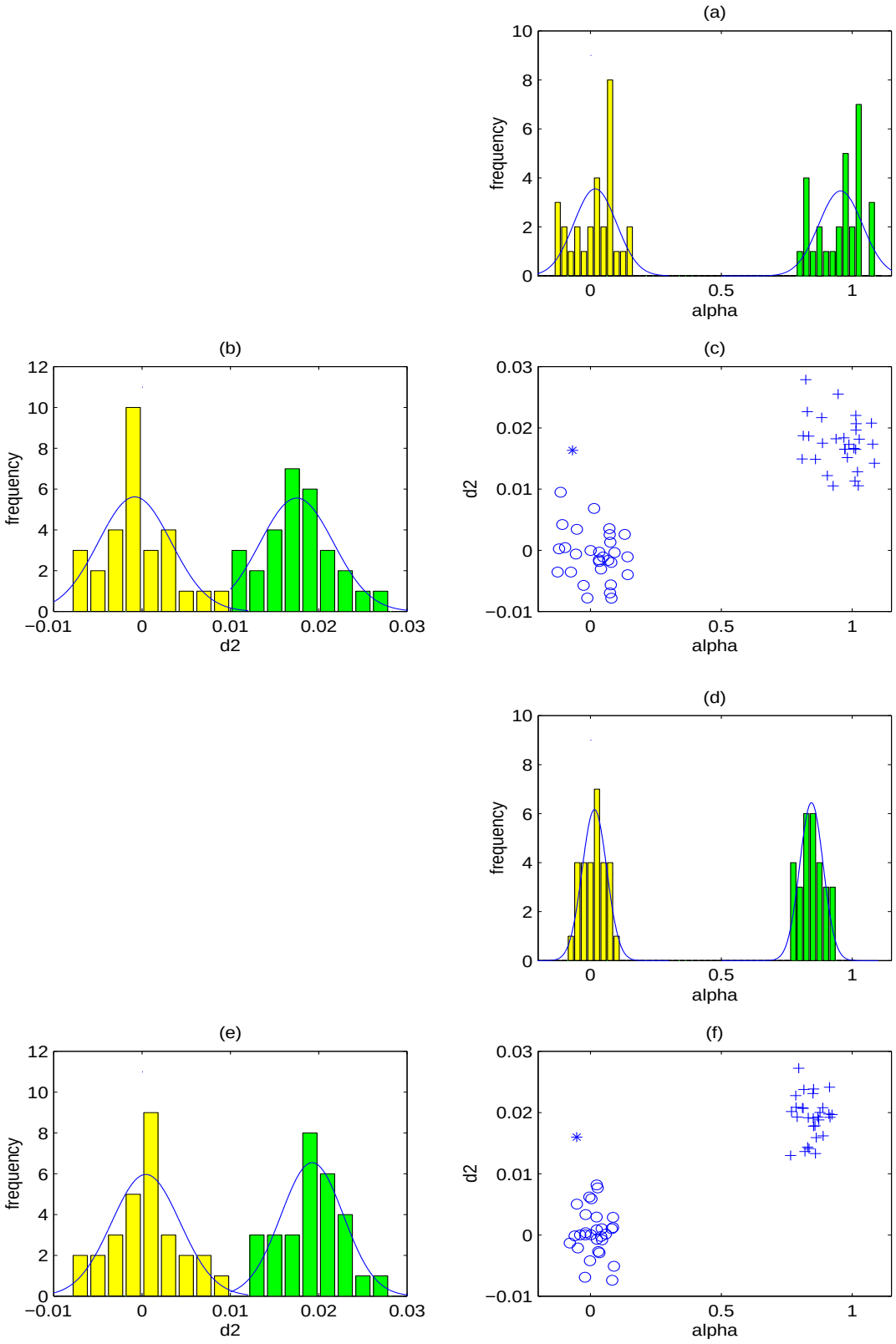

Figure 15: Exp 1: Estimates of α and d_2. Dark and +: forced proxies. Light and o: background proxies. $*$: historical data. (a)-(c) GFDL data. (d)-(f) NCAR1 data.

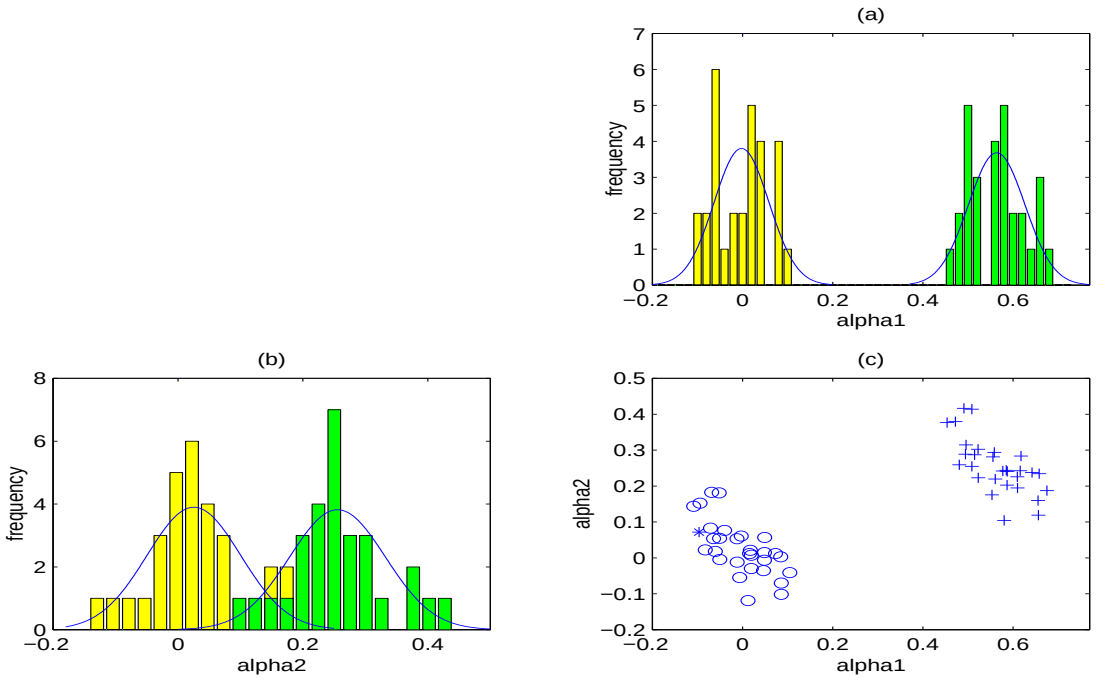

Figure 16: Exp 2: Estimates of α_1, α_2. Dark and +: proxies forced with $\alpha_1, \alpha_2 = (.65, 35)$. Light and o: background proxies.

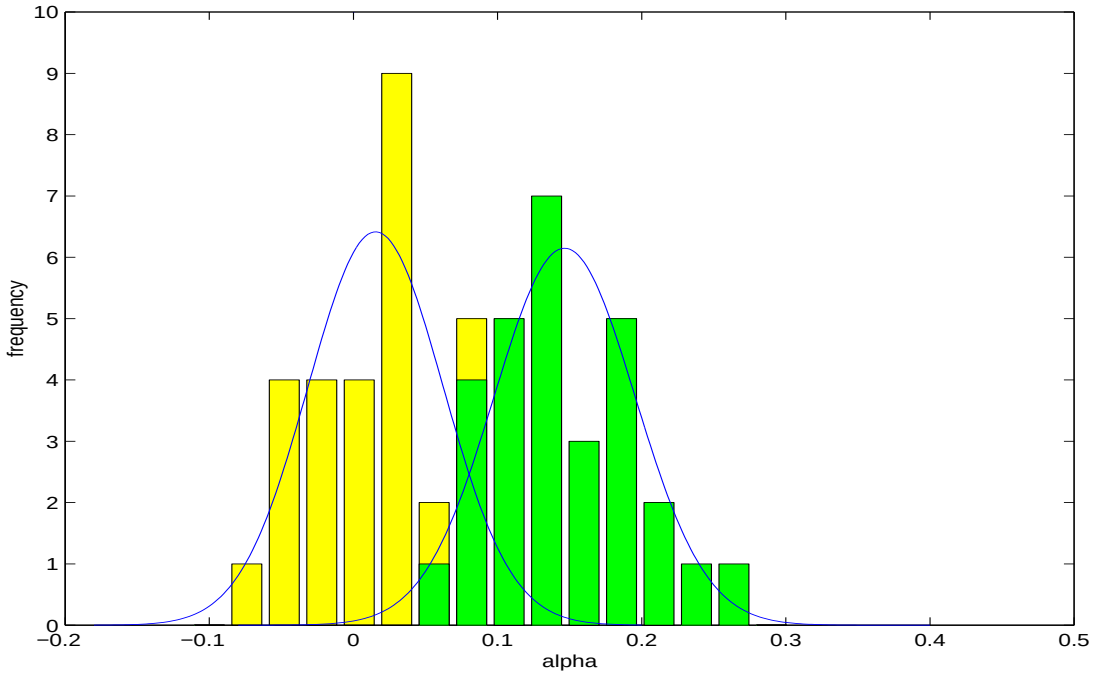

Figure 17: Exp 3: Estimates of α. Dark: proxies forced. Light: background proxies.

A Quasi-interpolation and scaling for decomposition of climate model output

A.1 The reproducing kernels

To establish notation for later, we give the four reproducing kernels R_1, R_2, R_3, R_4 of Equation (8). More details may be found in Luo et al. (1998). Let L be the $n_1 \times (n_1 - 2)$ matrix

$$L = \begin{pmatrix} 1 & -2 & 1 & 0 & 0 & \cdots & 0 \\ 0 & 1 & -2 & 1 & 0 & \cdots & 0 \\ \vdots & & & & & & \vdots \\ 0 & 0 & 0 & \cdots & 1 & -2 & 1 \end{pmatrix}. \tag{1}$$

then $J_1(f_1) = \|Lf_1\|^2$ and the reproducing kernel for J_1 is the $n_1 \times n_1$ matrix with t, τth entry $R_t(t,\tau) = (L'L)^+_{t,\tau}$ of $(L'L)^+$, the Moore Penrose generalized inverse of $L'L$. An approximate reproducing kernel for $J_2(f_2)$, which we used here, is

$$R_s(P,Q) = \frac{1}{2\pi}[\frac{1}{2}q_2(z) - \frac{1}{6}], \tag{2}$$

where $z = cos(\gamma(P,Q))$, $\gamma(P,Q)$ is the angle between P and Q, and

$$\begin{aligned} q_2(z) &= \frac{1}{2}\{ln(1 + (\frac{2}{1-z})^{1/2})[12(\frac{1-z}{2})^2 - 4(\frac{1-z}{2})] \\ &\quad -12(\frac{1-z}{2})^{3/2} + 6(\frac{1-z}{2}) + 1\} \end{aligned}$$

(from Wahba (1981) formulas (3.3) and (3.4)). The exact reproducing kernel for $J_2(f_2) = \int_{\mathcal{S}}(\Delta f)^2 dP$ involves a Green's function for $\Delta\cdot\Delta$ and a closed form expression is not available. Further details are given in Wahba (1981), Wahba (1982*a*). The reproducing kernel for the one dimensional subspace spanned by ϕ is just $\phi(t)\phi(\tau)$. The reproducing kernels for $\mathcal{H}^v$, $v = 1, 2, 3, 4$, are defined and summarized in Table 6.

Table 6: Reproducing kernels for the four subspaces that contain the four nonparametric components in (6).

v	Reproducing Kernel
1	$R_1(t,P;\tau,Q) = R_t(t,\tau)$
2	$R_2(t,P;\tau,Q) = R_s(P,Q)$
3	$R_3(t,P;\tau,Q) = \phi(t)\phi(\tau)R_s(P,Q)$
4	$R_4(t,P;\tau,Q) = R_t(t,\tau)R_s(P,Q)$

Given c, note that $f_1(t) = \sum_{i=1}^n c_i\theta_1 R_t(t_i,t)$, $f_2(P) = \sum_{j=i}^n c_i\theta_2 R_s(P_i,P)$, $f_{\phi,2}(P) = \sum_{i=1}^n c_i\theta_2\phi(t_i)R_s(P_i,P)$, and $f_{12}(t,P) = \sum_{i=1}^n c_i\theta_4 R_t(t_i,t)R_s(P_i,P)$. It is also useful to recall that $J_\theta(\sum_i c_i Q_\theta(\cdot,\cdot;t_i,P_i)) = \sum_{i,j} c_i c_j Q_\theta(t_i,P_i;t_j,P_j)$, (the 'reproducing' property), see Wahba (1990)).

A.2 Quasi-interpolation on the sphere

Consider a variable defined over the sphere, in this study the average winter temperature for a particular year. Suppose we have climate model output at a grid of n_G locations (here $n_G = 1920$)

$$u_j = f(P_j) + \delta_j \quad j = 1, \cdots, n_G. \tag{3}$$

where $P_j \in \mathcal{S}$, the sphere. The δ_j now represents roundoff or truncation error. To quasi-interpolate the gridded u_j we first find f_θ, a function on the sphere, in the appropriate space, to minimize

$$\sum_{j=1}^{n}(u_j - f(P_j))^2 + \theta_2^{-1} J_2(f), \tag{4}$$

R_s is defined in (2). See Wahba (1981, 1990) for more details. f_θ has the representation

$$f_\theta(P) = d + \theta \sum_{j=1}^{n} c_j R_s(P, P_j), \tag{5}$$

where c is a vector of dimension n_G. Since the 'errors' are no longer random, but are (here being treated as) roundoff errors, θ_2 will be chosen so that $(\frac{1}{n_G}\sum_{j=1}^{n_G}(u_j - f(P_j))^2)$ matches an assumed standard deviation corresponding to roundoff error. The subroutine dsidr of RKPACK (Gu (1989)) was used to find d, c and θ. Then f_θ can be evaluated at the desired values of P to obtain the quasi-interpolated data. See Bates, Reames & Wahba (1993) for the effects of roundoff error in global interpolation methods. Roundoff error was assumed to be uniformly distributed between $\pm.5 \times 10^{-k}$, where k is the number of figures carried beyond the decimal point, giving a roundoff standard deviation of about $.3 \times 10^{-k}$. The GFDL and NCAR output was given respectively to $k = 2$ and $k = 3$ figures past the decimal point and these were the values used in the quasi interpolation. Note that that J_2 for quasi interpolation was deliberately chosen to agree with with J_2 in the ANOVA decomposition. Local piecewise linear interpolation (for example) is likely to induce more extraneous high frequency 'noise' into the carried over climate model output.

A.3 Decomposition of climate model data

As above, we expect the spline ANOVA model to fit the data points to a specified number of figures after the decimal. However, for roundoff error, the penalty terms in (6) will be small and the fitting procedure becomes numerically unstable, and there is no guarantee that there is a unique set of four θ's that will match the input data to a specified degree of accuracy. From equation (2.3.6) of Luo (1996), if it happens in the computational algorithm θ_4 increases much faster than θ_1, then the main effect for time will converge to zero.

One way of overcoming this is to enforce relations between the θ's by scaling arguments. We do this by re-define the reproducing kernels in Table 6 as follows: Let $\theta_1 = \lambda b_t$, $\theta_2 = \lambda b_s$, $\theta_3 = \lambda b_s b_\phi$, and $\theta_4 = \lambda b_t b_s$, where b_t, b_s, b_ϕ, and λ are positive real numbers. The representation in (8) does not change if we re-define the four reproducing kernels as shown in

Table 7: Scaled reproducing kernels for climate model output decomposition.

v	Reproducing Kernel
1	$R_1(t,P;\tau,Q) = b_t R_t(t,\tau)$
2	$R_2(t,P;\tau,Q) = b_s R_s(P,Q)$
3	$R_3(t,P;\tau,Q) = b_\phi b_s \phi(t)\phi(\tau) R_s(P,Q)$
4	$R_4(t,P;\tau,Q) = b_t b_s R_t(t,\tau) R_s(P,Q)$

Table 7. Let $b_t = 10^{-0.1}$ and $b_s = 10^{4.5}$, as in Luo et al. (1998). Both are chosen such that the trace of the marginal smoothers (Buja, Hastie & Tibshirani (1989)), $tr((R_1 + I/b_t)^{-1}R_1)/28$ and $tr((R_2 + I/b_s)^{-1}R_2)/1000$, are about .99. Here R_2 is the matrix obtained by evaluating $R_2(t,P;\tau,Q)$ at the observation points in space. This will ensure that $f_1(t)$ and $f_2(P)$ are in effect being smoothed only negligibly. b_ϕ is derived from the ranges of $f_2(P)$ and $f_{\phi,2}(P)$ in historical data. Specifically, the range for $f_2(P)$ and $f_{\phi,2}(P)$ are about $(-40, 40)$ and $(-0.2, 0.2)$ respectively. We let the ratio of $R_2(t,P;\tau,Q)$ to $R_3(t,P;\tau,Q)$ be equal to the square ratio of 80 and 0.4. That is,

$$\frac{1}{(\frac{1}{30}\sum_{t=1}^{30}\phi(t)^2)b_\phi} = (\frac{80}{0.4})^2.$$

This gives $b_\phi = 10^{-6.4766}$. After this formulation, the residual root mean square is a monotone function of λ and we increase λ until the root mean square residual is less than 0.3×10^{-2} for the GFDL datasets and is less than 0.3×10^{-3} for the NCAR datasets. This procedure will guarantee that the fitted values match the data points by at least two figures after the decimal for the GFDL datasets and three figures after the decimal for the NCAR datasets, and that the relative scales of the components remain realistic.

List of Tables

References

Barnett, T., Hegerl, G., Santer, B. & Taylor, K. (1998), 'The potential effect of GCM uncertainities and internal atmospheric variability on anthropogenic signal detection', *J. Climate* **11**, 659–675.

Bates, D., Reames, F. & Wahba, G. (1993), 'Getting better contour plots with S and GCVPACK', *Computational Statistics and Data Analysis* **15**, 329–342.

Bennett, A. (1992), *Inverse methods in physical oceanography*, Cambridge University Press, 346pp.

Bennett, A. (1997), 'Inverse methods and data assimilation', College of Oceanic And Atmospheric Sciences, Corvallis OR. Summer School Lecture Notes.

Bloomfield, P. & Nychka, D. (1992), 'Climate spectra and detecting climate change', *Climate Change* **21**, 275–287.

Buja, A., Hastie, T. & Tibshirani, R. (1989), 'Linear smoothers and additive models. (with discussion)', *The Annals of Statistics* **17**, 453–555.

Dee, D., Gaspari, G., Redder, C., Rukhovets, L. & daSilva, A. (1998), 'Maximum-likelihood estimation of forecast and observation error covariance parameters. part ii: Applications', *Monthly Weather Review* **in press**, xx–xx.

Erickson, D., Oglesby, R. & Marshall, S. (1995), 'Climate response to indirect anthropogenic sulfate forcing', *Geophys. Res. Lett.* **22**, 2017–2020.

Girard, D. (1998), 'Asymptotic comparison of (partial) cross-validation, GCV and randomized GCV in nonparametric regression', *The Annals of Statistics* **126**, 315–334.

Goody, R., Anderson, J. & North, G. (1998), 'Testing climate models: An approach', *Bull. Amer. Meteor. Soc.* pp. 2541–2549.

Gu, C. (1989), Rkpack and its applications: Fitting smoothing models, *in* 'Proceedings of the Statistical Computing Section', American Statistical Association, pp. 42–51.

Gu, C. & Wahba, G. (1993), 'Smoothing spline ANOVA with component-wise Bayesian confidence intervals', *Journal of Computational and Graphical Statistics* **2**, 97–117.

Haigh, J. (1996), 'The impact of solar variability on climate', *Science* **272**, 981–984.

Hasselmann, K. (1997), 'Multi-pattern fingerprint method for detection and attribution of climate change', *Climate Dyn.* **13**, 601–611.

Hasselmann, K. (1998), 'Conventional and Bayesian approach to climate-change detection and attribution', *Quart. J. Meteor. Soc.* **124**, 2541–2565.

Hegerl, G. & North, G. (1997), 'Comparisons of statistically optimal approaches to detecting anthropogenic climate change', *J. Climate* **10**, 1125–1133.

Hegerl, G., Hasselmann, K., Cubash, U., Mitchell, J., Roeckner, E., Voss, R. & Waszkewitz, J. (1997), 'Multi-fingerprint detection and attribution analysis of greenhouse gas, greenhouse gas-plus-aerosol and solar forced climate change', *Climate Dyn.* **13**, 613–634.

Hegerl, G., von Storch, H., Hasselmann, K., Santer, B., Cubash, U. & Jones, P. (1996), 'Detecting greenhouse-gas-induced climate change with an optimal fingerprint method', *J. Climate* **9**, 2281–2306.

Jones, P. (1994), 'Hemispheric surface air temperature variations: A reanalysis and in update to 1993', *J. Climate* **7**, 1794–1802.

Kaplan, A., Cane, M., Kushnir, Y., Clement, A., Blumenthal, B. & Rajagopalan, B. (1998), 'Reduced space optimal analysis for historical datasets: 136 years of atlantic sea surface temperatures', *J. Geophys. Res.* **103**, 18,567–18,589.

Kaplan, A., Kushnir, Y., Cane, M. & Blumenthal, M. (1997), 'Reduced space optimal analysis for historical datasets: 136 years of atlantic sea surface temperatures', *J. Geophys. Res.* **27**, 25,835–27,860.

Kimeldorf, G. & Wahba, G. (1970), 'A correspondence between Bayesian estimation on stochastic processes and smoothing by splines', *The Annals of Mathematical Statistics* **41**, 495–502.

Kimeldorf, G. & Wahba, G. (1971), 'Some results on Tchebycheffian spline functions', *Journal of Math. Anal. Applic.* **33**, 173–180.

Kooperberg, C. & O'Sullivan, F. (1996), 'Predictive oscillation patterns: A synthesis of methods for spatial-temporal decomposition of random fields', *Journal of the American Statistical Association* **91**, 1485–1496.

Leroy, S. (1998), 'Detecting climate signals: Some Bayesian aspects', *J. Climate* **11**, 640–651.

Leroy, S. (1999), 'Optimal detection of global warming using temperature profiles: Methodology', *J. Climate* **12**, 1185–1198.

Levine, R. & Berliner, L. (1999), 'Statistical principles for climate change studies', *J. Climate* **12**, 565–574.

Luo, Z. (1998), 'Backfitting in smoothing spline ANOVA', *The Annals of Statistics* **26**, 1733–1759.

Luo, Z., Wahba, G. & Johnson, D. (1998), 'Spatial-temporal analysis of temperature using smoothing spline ANOVA', *J. Climate* **11**, 18–28.

Manabe, S., Spelman, M. & Stouffer, R. (1992), 'Transient responses of a coupled ocean-atmosphere model to gradual changes of atmospheric CO_2. part II: seasonal response', *J. Climate* **5**, 105–126.

Manabe, S., Stouffer, R., Spelman, M. & Bryan, K. (1991), 'Transient responses of a coupled ocean-atmosphere model to gradual changes of atmospheric CO_2. part I: annual mean response', *J. Climate* **4**, 785–818.

Meehl, G., Washington, W., Erickson, D., Briegleb, B. & Jaumann, P. (1996), 'Climate change from increased CO2 and the direct and indirect effects of sulfate aerosols', *Geophys. Res. Lett.* **23**, 3755–3758.

Nelder, J. & Mead, R. (1965), 'A simplex method for function minimization', *The Computer Journal* **7**, 308–313.

North, G. & Stevens, M. (1998*a*), 'Detecting climate signals in the surface temperature record', *J. Climate* **11**, 563–577.

North, G. & Stevens, M. (1998*b*), 'Eof-based linear prediction algorithm:theory', *J. Climate* **11**, 3046–3056.

North, G., Kim, K.-Y., Shen, S. & Hardin, J. (1995), 'Detection of forced climate signals, Part I: Filter theory', *J. Climate* **8**, 401–408.

Nychka, D. (1988), 'Bayesian confidence intervals for smoothing splines', *J. Amer. Statist. Assoc.* **83**, 1134–1143.

Nychka, D. (1990), 'The average posterior variance of a smoothing spline and a consistent estimate of the average squared error', *Ann. Statist.* **18**, 415–428.

O'Sullivan, F. & Wahba, G. (1985), 'A cross validated Bayesian retrieval algorithm for non-linear remote sensing', *J. Comput. Physics* **59**, 441–455.

Polyak, I. (1996), 'Observed second-moment statistics in GCM verification problems', *J. Atmos. Sci.* **53**, 608–627.

Ramaswamy, V. & Chen, C. (1997), 'Linear additivity of climate response for combined albedo and greenhouse perturbations', *Geophys. Res. Lett.* **24**, 567–570.

Rao, C. (1973), *Linear Statistical Inference and Its Applications, 2nd ed.*, Wiley, 656 pp.

Santer, B., Cubasch, U., Mikolajewicz, U. & Hegerl, G. (1993), The use of general circulation models in detecting climate change induced by greenhouse gases, Technical Report 10, Program for Climate Model Diagnosis and Intercomparison.

Santer, B., Taylor, K., Wigley, T., Johns, T., Jones, P., Karoly, D., Mitchell, J., Oort, A., Penner, J., Ramaswamy, V., Schwarzkopf, M., Stouffer, R. & Tett, S. (1996), 'A search for human influences on the thermal structure of the atmosphere', *Nature* **382**, 39–46.

Santer, B., Taylor, K., Wigley, T., Penner, J., Jones, P. & Cubasch, U. (1995), 'Towards the detection and attribution of an anthropogenic effect on climate', *Climate Dyn.* **12**, 77–100.

Stevens, M. & North, G. (1996), 'Detection of the climate response to the solar cycle', *J. Atmos. Sci.* **53**, 2594–2608.

Stott, P. & Tett, S. (1998), 'Scale-dependent detection of climate change', *J. Climate* **11**, 3282–3294.

Tett, S., Mitchell, J., Parker, D. & Allen, M. (1996), 'Human influence on the atmospheric vertical temperature structure: Detection and Observations', *Science* **274**, 1170–1173.

von Storch, H. & Zwiers, F. (1999), *Statistical analysis in climate research*, Cambridge University Press, 528 pp.

Wahba, G. (1981), 'Spline interpolation and smoothing on the sphere', *SIAM Journal on Scientific and Statistical Computing* **2**, 5–16.

Wahba, G. (1982*a*), 'Erratum: spline interpolation and smoothing on the sphere', *SIAM Journal on Scientific and Statistical Computing* **3**, 385–386.

Wahba, G. (1982*b*), Variational methods in simultaneous optimum interpolation and initialization, *in* D. Williamson, ed., 'The Interaction Between Objective Analysis and Initialization', Atmospheric analysis and Prediction Division, National Center for Atmospheric Research, Boulder, CO, pp. 178–185.

Wahba, G. (1983), 'Bayesian confidence intervals for the cross-validated smoothing spline', *Journal of the Royal Statistical Society, Series B* **45**, 133–150.

Wahba, G. (1990), *Spline models for observational data*, SIAM CBMS-NSF Regional Conference Series in Applied Mathematics, Vol.59, 169 pp.

Wahba, G. (1998), Adaptive tuning, four dimensional variational data assimilation and representers in rkhs, Technical Report 1000, to appear Proceedings ECMWF Workkshop, Deptartment of Statistics, University of Wisconsin, Madison WI.

Wahba, G. & Luo, Z. (1997), 'Smoothing spline ANOVA fits for very large, nearly regular data sets, with application to historical global climate data', *Ann. Numer. Math.* **4**, 579–597.

Wahba, G., Wang, Y., Gu, C., Klein, R. & Klein, B. (1995), 'Smoothing spline ANOVA for exponential families, with application to the Wisconsin Epidemiological Study of Diabetic Retinopathy', *Ann. Statist.* **23**, 1865–1895. Neyman Lecture.

Wang, X. & Shen, S. S. (1999), 'Estimation of spatial degrees of freedom of a climate field', *J. Climate* **12**, 1280–1291.

Wigley, T., Jaumann, P., Santer, B. & Taylor, K. (1998), 'Relative detectability of greenhouse-gas and aerosol climate change signals', *Climate Dyn.* **14**, 781–790.

Zwiers, F. (1998), Climate change detection: A review of techniques and application, *in* H. von Storch, E. Raschke & G. Floser, eds, 'Anthropogenic Climate Change. Proceedings of the First GKSS Spring School on Environmental Research', Springer Verlag, New York.